
**LUIZ EDUARDO SILVA**

# STRUCTURAL CHANGES IN MICROFIBRILLATED CELLULOSE SUBMITTED TO REDISPERSION METHODS

**LAVRAS – MG**

**2020**

**LUIZ EDUARDO SILVA**

# STRUCTURAL CHANGES IN MICROFIBRILLATED CELLULOSE SUBMITTED TO REDISPERSION METHODS

Tese apresentada à Universidade Federal de Lavras, como parte das exigências do Programa de Pós- Graduação em Engenharia de biomateriais, área de concentração em Compósitos e Nanocompósitos Lignocelulósicos, para a obtenção do título de Doutor.

Dr. Gustavo Henrique Denzin Tonoli
Orientador

Dr. Alfredo Rodrigues de Sena Neto
e
Dr. Greggory Glen
Coorientadores

**LAVRAS - MG**
**2020**

**Ficha catalográfica elaborada pelo Sistema de Geração de Ficha Catalográfica da Biblioteca Universitária da UFLA, com dados informados pelo(a) próprio(a) autor(a).**

Silva, Luiz Eduardo.
Structural changes in microfibrillated cellulose submitted to redispersion methods / Luiz Eduardo Silva. - 2020.
67 p. : il.

Orientador(a): Gustavo Henrique Denzin Tonoli.
Coorientador(a): Alfredo Rodrigues Sena Neto, Gregory Glenn.
Tese (doutorado) - Universidade Federal de Lavras, 2020.
Bibliografia.

1. Cellulose nanofibrils. 2. Drying. 3. Redispersion in water. I. Tonoli, Gustavo Henrique Denzin. II. Sena Neto, Alfredo Rodrigues. III. Glenn, Gregory. IV. Título.

**LUIZ EDUARDO SILVA**

# STRUCTURAL CHANGES IN MICROFIBRILLATED CELLULOSE SUBMITTED TO REDISPERSION METHODS

# MUDANÇAS ESTRUTURAIS EM CELULOSE MICROFIBRILADA SUBMETIDA A MÉTODOS DE REDISPERSÃO

Tese apresentada à Universidade Federal de Lavras, como parte das exigências do Programa de Pós- Graduação em Engenharia de biomateriais, área de concentração em Compósitos e Nanocompósitos Lignocelulósicos, para a obtenção do título de Doutor.

Aprovada em 10 de agosto de 2020.
Dr. João Moreira Neto, UFLA
Dr. Saulo Rocha Ferreira, UFLA
Dr. Jeffrey Youngblood, Purdue University
Dr. William Hart-Cooper, University of California

PhD. Gustavo Henrique Denzin Tonoli
Orientador

PhD. Alfredo Rodrigues de Sena Neto
e
PhD. Greggory Glen
Coorientadores

**LAVRAS - MG**
**2020**

# AGRADECIMENTOS

Foi uma jornada árdua, com um grande crescimento acadêmico e pessoal. Mas não sozinho. Não caminhei sozinho, muito menos cresci sozinho. Por isso, não poderia entregar este documento sem antes sinceramente agradecer algumas pessoas.

Primeiramente e principalmente o meu mais sincero “obrigado” vai para meu orientador, Gustavo. Poderia filosofar, agradecer deidades, família ou quem fosse, mas essa etapa não teria se concluído se não fosse por ele. Por todas as oportunidades, orientação, atenção e incansável paciência, o agradeço!

Em segundo o meu companheiro Vlad. Se graças ao Gustavo eu consegui crescer academicamente, sem o Vlad não haveria crescimento pessoal. Uma pessoa ímpar. Foi meu sustento ao longo de toda a jornada com incondicional apoio, amor e também uma imensa dose de paciência. Esse título é tanto seu quanto meu.

Quem me introduziu à ciência não poderia faltar aqui. Dulcinéia de Carvalho. Alguém que não me canso de agradecer e levarei para toda a vida como não somente minha primeira orientadora, mas também uma querida amiga. Mais um ser de luz que entrou em minha vida e sem a qual não estaria aqui.

Ao pessoal do lab nano. De todas as eras que participei, sem exceções. São a personificação do companheirismo e auxílio ao próximo. Conquistamos títulos juntos, sofremos juntos, rimos juntos. Rimos mais do que deveria em muitas ocasiões. Mas foi necessário. Foi muito necessário como a presença de cada um tanto individualmente, como a soma de todos. Só tenho a agradecer aos meus queridos colegas: Allan, Alison, Lívia, Luiza, Lays, Matheus, Mário, Jordão, Maressa, Breno, Rafa e muitos outros que já passaram por lá e deixaram sua marca. Também aos meus alicerces externos ao laboratório: Guga, Luiz Otávio, Cris, Clarissa, Gustavo, Saulo, todos meus incríveis amigos que fiz na CTM e na Engenharia Florestal.

Especialmente, minha família. Todos que agradeci até agora haviam me ajudado e guiado por esses 10 anos de formação, mas os 20 anteriores a isso se devem à minha família. Somos um produto do que vivemos e vivenciamos. Me orgulho de ser quem eu sou e de quem me tornei. Portanto, à todos os membros de minha família, em todas as esferas, eu agradeço de todo meu coração. Desde meu núcleo mais próximo, como meus pais e minhas irmãs, até minhas tia(o)s e prima(o)s maravilhosos que tenho.

Por fim, agradeço à UFLA, o Programa de Pós-graduação em Engenharia de Biomateriais e todo o governo, obviamente anterior ao vigente, que me possibilitou os estudos.

Se engana aquele que acha que o futuro se constrói sem uma educação de verdadeira qualidade. Meu muitíssimo obrigado!

O presente trabalho foi realizado com apoio da Coordenação de Aperfeiçoamento de Pessoal de Nível Superior – Brasil (CAPES) – Código de Financiamento 001, e por isso sou imensamente grato.

## RESUMO

Celulose microfibrilada (CMF) representa um material de grande interesse para diversas indústrias, como a de compósitos, farmacêuticas, de eletrônicos e muitas outras. Devido a sua estrutura e tamanho, possui propriedades diferenciadas em relação à macrofibras. Porém, a secagem desse material ocasiona em agregação das partículas, o que faz com que a mesma perca suas características únicas. Portanto, o trabalho busca elucidar diferentes abordagens da secagem das CMF e apresentar possíveis métodos de secagem. No primeiro artigo apresentado, a relação entre a quantidade de ciclos de secagens e a temperatura, e sua consequente influência na estrutura das CMF foi estudado. Os resultados mostram que o maior número de secagens e uma maior temperatura causam uma maior agregação nas CMF, crescimento das partículas, perda de estabilidade em água e redução na resistência mecânica. O tratamento seco somente uma vez a temperatura ambiente (20°C) foi o mais promissor, com morfologia e tamanho de partícula próximas a CMF não-seca; o que torna este tratamento o mais indicado, quando se utilizar o método de secagem em estufa. No segundo artigo foi analisada a presença de aditivos para auxiliar a redispersão de CMF secas por liofilização. A não utilização de aditivos obteve o pior resultado, com grande formação de agregados, maior tamanho de partícula e perda considerável em propriedades mecânicas. A presença de cloreto de sódio auxiliou a redispersão, porém ainda apresentou uma considerável diferença em relação às CMF não-secas. O uso do surfactante dodecil sulfeto de sódio garantiu a redispersão ao ponto de ser comparada, em relação à morfologia e estrutura, às CMF não-secas. Uma quantidade vestigial do surfactante fez com que as propriedades mecânicas superassem as CMF não-secas, fazendo com que o tratamento não só realizasse a redispersão como a interação entre CMF e o surfactante ocasionasse em melhora das propriedades.



**Palavras-chave**: Secagem em estufa. Liofilização. Agregação. Hornificação. Cloreto de sódio. Dodecil sulfato de sódio.

## ABSTRACT

Microfibrillated cellulose (MFC) represents a material of great interest for several industries, such as composites, pharmaceuticals, electronics and many others. Due to its structure and size, it has different properties compared to macrofibers. However, drying causes aggregation of these particles, which makes it lose its unique characteristics. Therefore, the present study seeks to elucidate different approaches to MFC drying and to present possible drying methods. In the first article presented, the relationship between the number of drying cycles and temperature, and their consequent influence on the MFC structure was studied. The results show that the greater number of drying cycles and a higher temperature cause a greater aggregation in the MFC, growth of the particles, loss of stability in water and loss of mechanical properties. Once-dried at room temperature (20°C) was the most promising, with morphology and particle size close to never-dried MFC; which makes this treatment the most suitable when using the oven-drying method. In the second article, the presence of additives to aid redispersion of freeze-dried MFC was analyzed. The sample dried with no additive obtained the worst result, with great formation of aggregates, larger particle size and considerable loss in mechanical properties. The presence of sodium chloride helped the redispersion, but it still showed a considerable difference in relation to never-dried MFC. The use of the surfactant sodium dodecyl sulfate has assured redispersion to the point of being compared, in terms of morphology and structure, to never-dried MFC. Trace amount of the surfactant caused the mechanical properties to surpass the never-dried MFC, causing the treatment not only to carry out the redispersion but also the interaction between MFC and the surfactant to improve the properties.



**Keywords**: Oven-drying. Freeze-drying. Aggregation. Hornification. Sodium chloride. Sodium dodecyl sulfate.

**SUMÁRIO**

# INTRODUCTION

Cellulose is the most abundant biopolymer existent in the planet and, due to its low cost and renewable source, it is a product that easily became marketable. Since its source comes mostly from vegetable biomass, easily obtained, cellulose is currently present in several segments of the industrial chains, such as pharmaceutical, construction and electronics. And, with help from nanotechnology, cellulose fibers can be turned into microfibrillated cellulose (MFC) that will create new products with unique properties, which macrofibers were unable to produce themselves.

However, there is still an obstacle in the commercialization of these nanoscale fibers. Drying is an irreversible or partially reversible process that results in MFC agglomeration, making the particles larger, which causes them to lose their nanoscale properties, such as transparency and high tensile strength. Currently MFC commercialization occurs in water suspensions to avoid drying and subsequent agglomeration. The development of a drying process that would allow a successful redispersion of the material would be of great interest not only for companies, but also for the scientific community.

Currently, there are several ways of chemical and physical modification, such as the functionalization of cellulose carboxyl groups, which, although effective, are treatments that result in a material chemically different from the original. However, the use of additives that do not chemically modify cellulose may be a viable alternative, if it is a low-cost additive. Physical treatments are also feasible; however, there is usually a change in MFC crystalline structure which leads to changes in their properties, such as mechanical strength, hygroscopicity and permeability. Thus, the drying and redispersion process, that could maintain the integrity of cellulose, becomes a challenge. Several studies have addressed MFC redispersion theme, but factors such as success in redispersion, optimal temperature, use of additives and the combination of these factors have yet to be elucidated.

Therefore, the present study focuses on elucidating the possible structural, physical and morphological modifications of cellulose micro/nanofibrils as well as proposing new methods of redispersion mediated by different temperatures and addition of low-cost salts and surfactants.

# OBJECTIVES

1. Study the effect of MFC morphological and structural changes caused by drying temperature and number of drying cycles;

2. Evaluate the use of sodium chloride and sodium dodecyl sulfate as additives and assess the ability to produce redispersible MFC samples.

# PART I - BACKGROUND

## 1 Cellulose micro/nanofibrils structure

Cellulose is one of the three main components of plant biomass, along with lignin and hemicelluloses (SJÖSTRÖM, 1981). Although the most abundant source is biomass (ZHAO *et al.*, 2017; HUBER *et al.*, 2012), cellulose can also be found in bacteria (CAZÓN; VELAZQUEZ; VÁZQUEZ, 2020) and tunicates, which is the only animal producing cellulose (ZHAO *et al.*, 2017). Biomass is largely used due to its availability, low-cost production, renewable source, biodegradable and many other features that makes it commercially viable (GUIMARAES JUNIOR; TEIXEIRA; TONOLI, 2018; ZHAO *et al.*, 2017; TONOLI *et al.*, 2016; HUBER *et al.*, 2012;).

The structure of plant fiber begins on itself, on a macroscale, and can be divided into layers. In the thickest layer of the cell wall, the secondary layer, is where the highest concentration of cellulose can be found. In it, cellulose is arranged in microfibrils wrapped in a matrix of amorphous cellulose, lignin and hemicelluloses (TOBA; YAMAMOTO; YOSHIDA, 2013). Cellulose microfibrils are 3 to 20 nm in diameter and up to 1 μm in length (IOELOVICH, 2008; SJÖSTRÖM, 1981), oriented towards the axial direction of the fiber, forming acute angles, to maximize the tensile strength (IOELOVICH, 2008).

Due to its chemical constitution and degree of polymerization, cellulose is responsible for the tensile strength of vegetable fibers (HUBER *et al.*, 2012). Cellulose is composed of a linear chain with repeated glucose units strongly linked by β-(1,4) bonds and numerous hydroxyl groups on its surface. The linearity of cellulose chains and arrangement of hydroxyl groups make the formation of crystals possible; and their crystallinity can be correlated with physical properties of the lignocellulosic material (TOBA; YAMAMOTO; YOSHIDA, 2013). Cellulose is the only constituent that contributes to crystallinity, while hemicellulose and lignin are amorphous counterparts (KELLEY; RIALS; GLASSER, 1987).

Cellulose chains can not only be linked laterally, but also stacked. Hydroxyls are located to the sides and make hydrogen bonds with other parallel chains, while hydrogen atoms are directed to the poles, by electrostatic repulsion, which causes the “stacking” to be carried out by hydrophobic secondary bonds, providing cellulose an intrinsically anisotropic structure (SILVEIRA *et al.*, 2016; YAMANE *et al.*, 2006). Figure 1 shows hydroxyl and hydrogen groups separation by equatorial and axial positions of the molecule showcasing cellulose anisotropy.

Figure 1: Cellulose chain structure and its anisotropy.

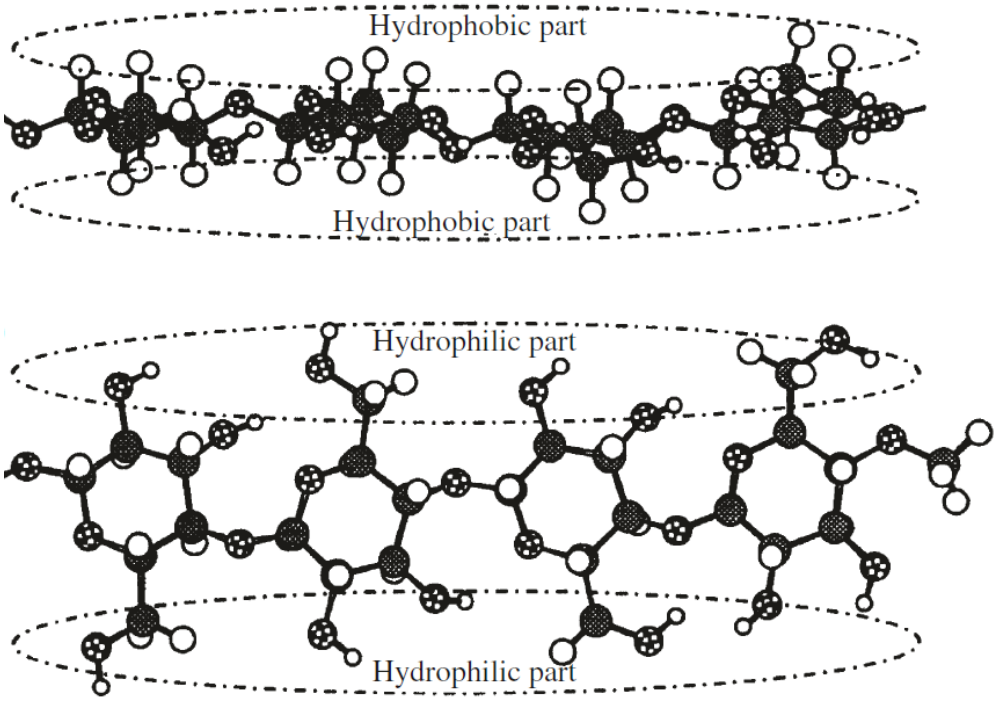


Source: Yamane *et al.* (2006)

Cellulose can be found in 4 different polymorphs: I, II, III and IV (XU; SHI; WANG, 2013). Cellulose I is considered native (KHAZRAJI; ROBERT, 2013) and has two allomorphs: cellulose Iβ, mostly found in plant cell wall, and cellulose Iα, which enriches some microbes, such as bacteria (CAZÓN; VELAZQUEZ; VÁZQUEZ, 2020; KHAZRAJI; ROBERTT, 2013). The difference between the allomorphs Iα and Iβ is in hydroxyl position that causes the unit cell to package differently, which is triclinic for Iα and monoclinic for Iβ (HUBER *et al.*, 2012; WERTZ; BÉDUÉ; MERCIER, 2010).

Starting from the vegetable fiber, it is possible to obtain fibers with nanoscale dimensions close to natural microfibrils. One of the easiest and most common routs is the mechanical (SILVA *et al.*, 2019; GUIMARÃES JÚNIOR *et al.*, 2015; TONOLI *et al.*, 2012). Through this route, fibers dispersed in water are subjected to a strong mechanical shear that causes the cellulose to be individualized, or microfibrillated (MFC). The micro/nanofibrils term is used because it covers a wide class of diameters that can be from a few nanometers to a few micrometers (TONOLI *et al.*, 2012). This happens due to the mechanical severing of some hydrogen bonds, which links one fibril to another, leaving, however, few intact regions with dimensions close to the original fibers. It is possible to further reduce fiber diameter, but prolonged exposure to mechanical fibrillation leads to a reduction in cellulose degree of polymerization, which in turn reduces mechanical strength (BENÍTEZ; WALTHER, 2017).

Reducing the size of the fibers to MFC can improve several properties, such as optical, mechanical and barrier (ZOU *et al.*, 2020; ARANTES *et al.*, 2019; KARASU *et al.*, 2018). Also, MFC is a nanoscale material with a high surface area, due to its many individual nanofibrils (IOELOVICH, 2008) that helps it binding with matrices, other polymers, or itself, to form resistant films (ARANTES *et al.*, 2019; GUIMARAES JUNIOR; TEIXEIRA; TONOLI, 2018; CLARO *et al.*, 2018).

## 2 Drying process and effect upon MFC

### *2.1 Oven-drying*

The oven-drying process involves removing water from the sample with the aid of temperature. In these cases, drying takes place in three stages with different drying rates (ZIMMERMAN *et al.*, 2016; PENG *et al.*, 2012; SCHERER, 1986). The first stage happens at a constant rate and acts to reduce the volume of free water present in the sample. During the first phase, the sample loses water and there is an increase MFC concentration. When the sample is concentrated, MFC movement becomes restricted. As a result, MFC closer to the surface have their surfaces exposed and drying enters its second stage. On this second phase, evaporation rate is reduced and water removal occurs mainly on the exposed MFC surface (PENG *et al.*, 2012). During this stage, water vapor is formed inside the dispersion and carries moisture out to the surface of the fibers, where it will be removed. Because of this diffusion process, MFCs begin to come closer due to restricted space and little mobility (ZIMMERMAN *et al.*, 2016). When the water transfer from inside the dispersion to its surface is less than the water diffused on the surface, drying enters its third stage (PENG *et al.*, 2012). During the last stage, drying process happens exclusively within the dispersion and MFCs are drawn near to the point of multiple hydrogen bonding, thus causing irreversible MFC aggregation (ZIMMERMAN *et al.*, 2016; PENG *et al.*, 2012). Figure 2 shows the oven-drying stages. After MFC drying and aggregating, even if resuspended, the fibrils will remain irreversibly bound.

Figure 2: Oven-drying stages: I) constant drying rate, II) first falling rate; and III) Second falling rate.

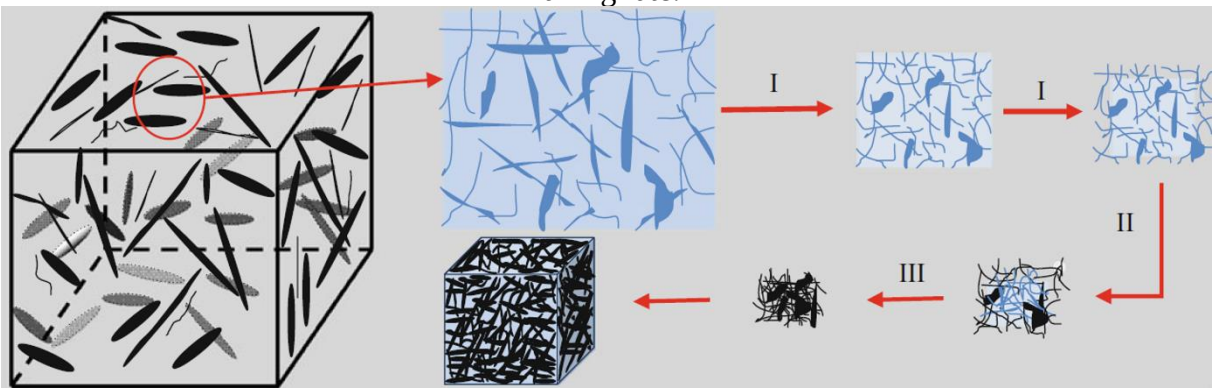


Source: Peng *et al.* (2012)

Nevertheless, not only the drying process, but also the temperature used during the process, interferes with MFC aggregation. High temperature drying is known as hornification (ZIMMERMAN *et al.*, 2016). Hornification is the process in which additional hydrogen bonds are formed in the cellulose that are not broken during rehydration (EYHOLZER *et al.*, 2010). Although there are studies that use it to strengthen fibers for reinforcement (BALLESTEROS *et al.*, 2017), when working with nanoscale fibers, the aggregation lowers surface area, which compromises physical-mechanical properties (GARCÍA-IRUELA *et al.*, 2019). The degradation temperature of lignocellulosic components ranges from 180°C for hemicelluloses to 250°C for lignin and cellulose (MO *et al.*, 2020), and these values can be higher if subjected to an inert atmosphere (CHEN *et al.*, 2019). Therefore, it is essential that the drying of lignocellulosic materials takes place at temperatures below its constituents' degradation point.

*2.2 Freeze-drying*

Freeze-dried products are of great interest in several industries, such as pharmaceuticals, packaging and paper due to a high resistance-to-weight ratio and high porosity (HAN *et al.*, 2013). Freeze-drying ensures better MFC dispersion, depending on the concentration (Figure 3), making several studies opt for this drying technique (THAI *et al.*, 2020; ZHANG *et al.*, 2019; MEDINA; CAROSIO; BERGLUNG, 2019). According to Han *et al.* (2013), high MFC concentration reduces the gap between fibrils, which in turn form hydrogen bonds with adjacent MFC, forming lamellar structures. Another advantage is the tendency of non-coalescence of fibers during drying, as occurred during oven-drying (PENG *et al.*, 2012), which makes freeze-drying the most used process for drying MFC, and producing aerogels, in laboratory (WANG *et al.* 2019).

Freeze-drying is a process that requires preparation before drying itself takes place. Therefore, it happens in two stages: freezing the sample and drying at low temperatures and vacuum, lyophilization (PENG *et al.* (2012). During the freezing stage, the particles dispersed in the suspension organize themselves according to the freezing front (MEDINA; CAROSIO; BERGLUNG, 2019; ANTONINI *et al.*, 2019; HAN *et al.*, 2013). This stage has a decisive role in the final characteristics of the material (WANG *et al.* 2019). Figure 3 exemplifies the difference in the morphology of samples with different concentrations subjected to freezing.

Figure 3: Dependence of concentration on sample morphology after freeze-drying.

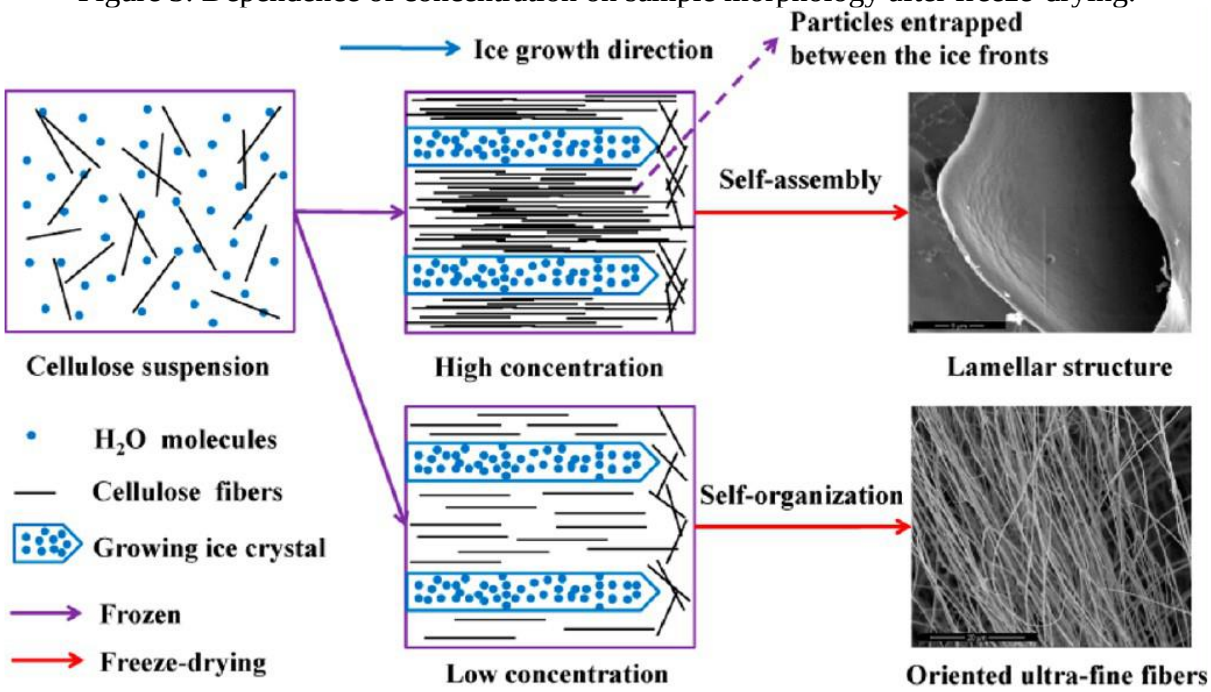


Source: Han *et al.* (2013)

Like oven-drying, freeze-drying occurs in 3 well-defined steps (ZIMMERMAN *et al.*, 2016; PENG *et al.*, 2012). However, the lyophilization process is completely different from the previous one. The first step is freezing. In this step, MFC are separated from the water, which will form ice crystals in the sample. The first drying stage (second stage) will sublimate the ice crystals. Due to the low pressure, the water is able to pass from ice to vapor, without liquefying. However, there is a portion of water linked to MFC that does not solidify. This portion of water is removed on the second drying stage, and final step. After removing the ice crystals, the water attached to the fiber surface is removed by heating the sample under vacuum. This stage can form aggregates due to unintentional chain approximation (PENG *et al.*, 2012). However, several factors can be regulated to obtain specific properties or structures for MFC, such as controlled porosity or even fiber alignment (WANG *et al.*, 2019). With high porosity, an ultra-

light material can be obtained, ideal for thermal insulation use, for example (THAI *et al.*, 2020; WANG *et al.*, 2019).

*2.3 Other methods*

Besides oven and freeze-drying, there are two other methods worth mentioned in terms of drying MFC. That is spray and supercritical drying.

Supercritical drying involves the use of fluids in its supercritical state, which endows them with both liquid and gas properties, such as compressibility and dissolution of solutes (ZIMMERMAN *et al.*, 2016). The diffusivity of the supercritical fluid facilitates solvent removal from the solid, preserving its structure. Normally, ethanol or acetone is used as a solvent instead of water to ease solvent extraction (DARPENTIGNY *et al*., 2020). Because of the high-cost from the high-pressure resistant equipment, usually $CO_2$ is the most used fluid due to its low temperature handling, low viscosity and no condensation into a liquid (DARPENTIGNY *et al.*, 2020; MATSUYAMA *et al.*, 2019; ZIMMERMAN *et al.*, 2016). MFC dried with supercritical $CO_2$ produces a light-weight and highly porous material called aerogel. While foams are usually made by freeze-drying the samples, aerogels are prepared by supercritical drying (MARTOIA *et al.*, 2016).

Another well-known method used is spray-drying. It is a consolidated method largely used in food, pharmaceutical, ceramic, and chemical industries (PENG *et al.*, 2012). This method is capable of controlling particle size of the sample, making it a desirable technique to be used in multiple products (WANG *et al.*, 2016). However, the production of spray-dried MFC needs to be carefully thought out, because cellulose is a highly hygroscopic material that could adhere onto the equipment surface or aggregate, and thus demands higher temperatures and lower feeding rate into the spray-drier (KOLAKOVICH *et al.*, 2012). Another problem is the possible clogging of the nozzle while drying highly viscous materials, limiting once again MFC at higher concentrations. That way, larger amounts of spray-dried MFC is unjustified, unless the use in high-end materials.

## 3 Additives to enhance redispersion

As much as careful drying may facilitate the redispersion of MFC in water, aggregate formation is still a hindrance. The hornification process that takes place during drying causes irreversible hydrogen bonds generating aggregates. Therefore, the main action to be taken during drying is to lessen these connections from occurring.

When cellulose chains interact, or even the concentration of the suspension is drastically increased, contact between them is made and hydrogen bonding can happen (HUBBE *et al.*, 2017). To reduce this occurrence, additives can be used before drying, to facilitate its subsequent redispersion (HUBBE *et al.*, 2017; MISSOUM; BRAS; BELGACEM, 2012). To block cellulose binding sites without changing the properties of the final material, it is necessary to use an additive that has an affinity with these binding sites, and which is easily extractable during redispersion. As an example, figure 4 shows the blocking of hydrogen bonds between cellulose chain performed by dissociated ions of sodium chloride. Ions are a good option for blocking hydrogen bonding. Ionic compounds, such as common table salt, are ideal to be used in MFC dispersion because they are products of high abundance, extremely cheap and does not permanently bond with cellulose. Missoum, Bras, and Belgacem (2012) investigated the addition of sodium chloride in suspension of cellulose nanofibrils before drying. The authors found a correlation between the use of NaCl and better nanofibril redispersibility. However, no structural and mechanical investigation has been done to assess the redispersed nanofibrils quality.

Figure 4: Hydrogen bond blockage promoted by dissolved sodium chloride ions.

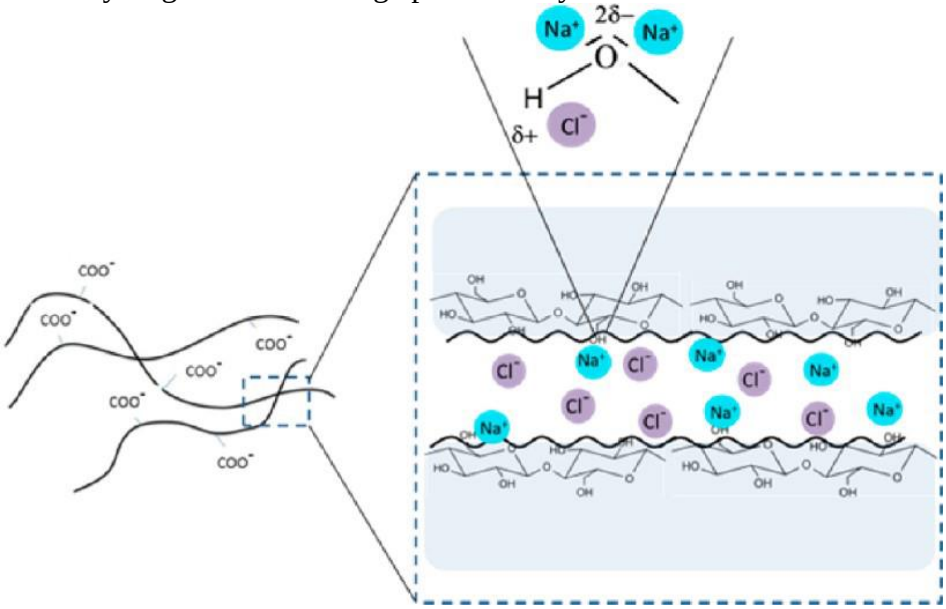


Source: Missoum, Bras and Belgacem (2012)

Surfactants are a viable choice due to cellulose amphiphilic nature (SILVEIRA *et al.*, 2016). In this sense, cellulose presents both positive and negative sites that could be used for bonding. Sodium dodecyl sulfate (SDS), or commercially known as sodium lauryl sulfate, is a common ionic surfactant used in several products (LO *et al.*, 2014). In high concentration, SDS

is able to facilitate temporary cross-link formation, caused by multiple linking sites on the micelle (LO *et al.*, 2014) and the bridging effect from two SDS molecules and cellulose chains (PATRUYO; MÜLLER; SÁEZ, 2002), making the dispersion maintain its shape during drying. However, as far as the authors know, SDS has not yet been used to aid in MFC redispersion.

Thus, the present study aims to better understand and assess oven-drying at multiple cycles as well as freeze-drying with help from additives, and analyze the aggregation process happening in both cases.

## CONSIDERATIONS

After thorough search on the literature, it can be seen that MFC redispersion is still in discussion. Several issues need to be decided in order to produce redispersible cellulose. The first one is which method is going to be applied. Different methods can produce different morphologys and have different costs. At this manuscript, oven and freeze-drying were chosen to be analyzed. Secondly, drying temperature is a parameter that can interfere in cellulose structure and final properties, and thus, it needs to be fully understood. Along with temperature, drying cycles is an interesting parameter correlated to re-use of MFC. Therefore, the first paper aims to elucidate the combination of both parameters. Another possibility is the use of additives. On the second paper, freeze-drying was decided to use, a more controlled technique, with two additives: sodium chloride and sodium dodecyl sulphate, and their comparison with never-dried and dried without any additive. Thus, both papers tackle a different aspect of MFC drying and redispersion, applying novel ideas.

## REFERENCES


ANTONINI, C. *et al*. **Ultra-Porous Nanocellulose Foams: A Facile and Scalable Fabrication Approach**. Nanomaterials, 9, 1142. 2019.

ARANTES, A. N. C. *et al.* **Bio-based thin films of cellulose nanofibrils and magnetite for potential application in green electronics**. Carbohydrate Polymers, 207, 100–107. 2019.

BALLESTEROS, J. E. M. *et al*. **Potential of the hornification treatment on eucalyptus and pine fibers for fiber-cement applications**. Cellulose, 24, 2275-2286. 2017.

BENÍTEZ, A. J.; WALTHER, A. **Cellulose nanofibril nanopapers and bioinspired nanocomposites: a review to understand the mechanical property space**. J. Mater. Chem. A., 31. 2017.

CAZÓN, P.; VELAZQUEZ, G.; VÁZQUEZ, M. **Characterization of mechanical and barrier properties of bacterial cellulose, glycerol and polyvinyl alcohol (PVOH) composite films with eco-friendly UV-protective properties**. Food Hydrocolloids, 99, 105323. 2020.

CHEN, W. *et al*. **Torrefaction, pyrolysis and two-stage thermodegradation of hemicellulose, cellulose and lignin**. Fuel, 258, 116168. 2019.

CLARO, P. I. C. *et al*. **Curaua and eucalyptus nanofibers films by continuous casting: Mechanical and thermal properties**. Carbohydrate Polymers, 181, 1093–1101. 2018.

DARPENTIGNY, C.; NONGLATON, G.; BRAS, J. AND JEAN, B. **Highly absorbent cellulose nanofibrils aerogels prepared by supercritical drying**. Carbohydrate Polymers, 229, 115560. 2020.

EYHOLZER, C. *et al*. **Preparation and characterization of water-redispersible nanofibrillated cellulose in powder form**. Cellulose 17, 19–30. 2010.

GARCÍA-IRUELA, A. *et al*. **Effect of vacuum/pressure cycles on cell wall composition and structure of poplar wood**. Cellulose, 26, 8543–8556. 2019.

GUIMARÃES JÚNIOR, M. *et al*. **Preparation of cellulose nanofibrils from bamboo pulp by mechanical defibrillation for their applications in biodegradable composites**. Journal of Nanoscience and Nanotechnology, 15, 1–18. 2015.

GUIMARAES JUNIOR, M.; TEIXEIRA, F. G. AND TONOLI, G. H. D. **Effect of the nano-fibrillation of bamboo pulp on the thermal, structural, mechanical and physical properties of nanocomposites based on starch/poly (vinyl alcohol) blend**. Cellulose. 25 (3), 1823 – 1849. 2018.

HAN, J. *et al*. **Self-assembling behavior of cellulose nanoparticles during freeze-drying: effect of suspension concentration, particle size, crystal structure, and surface charge**. Biomacromolecules, 14, 1529−1540. 2013.

HUBER, T. *et al*. **A critical review of all-cellulose composites**. J Mater Sci, 47, 1171–1186. 2012.

IOELOVICH, M. **Cellulose as a nanostructured polymer: a short review**. BioResources 3(4), 1403-1418. 2008.

KARASU, F. *et al*. **Organic-Inorganic Hybrid Planarization and Water Vapor Barrier Coatings on Cellulose Nanofibrils Substrates**. Front. Chem., 21. 2018.

KHAZRAJI, A. C.; ROBERT, S. **Interaction effects between cellulose and water in nanocrystalline and amorphous regions: a novel approach using molecular modeling**. Journal of Nanomaterials, 1-10. 2013.

KELLEY, S. S., RIALS, T. G. e GLASSER, W. G. **Relaxation behavior of the amorphous components of wood**. Journal of Materials Science, 22(2), 617–624. 1987.

KOLAKOVIC, R. *et al*. **Spray-dried nanofibrillar cellulose microparticles for sustained drug release**. International Journal of Pharmaceutics, 430, 47-55. 2012.

LO, J. *et al*. **Interaction between Hydrophobically Modified 2-Hydroxyethyl Cellulose and Sodium Dodecyl Sulfate Studied by Viscometry and Two-Dimensional NOE NMR Spectroscopy**. J. Phys. Chem. B, 118, 6922−6930. 2014. dx.doi.org/10.1021/jp500355n

MARTOÏA, F. *et al*. **Cellulose nanofibril foams: Links between ice-templating conditions, microstructures and mechanical properties**. Materials & Design, 104, 376 – 391. 2016.

MATSUYAMA, K. *et al*. **Antibacterial and antifungal properties of Ag nanoparticle-loaded cellulose nanofiber aerogels prepared by supercritical $CO_2$ drying**. The Journal of Supercritical Fluids, 143, 1-7. 2019.

MEDINA, L.; CAROSIO, F.; BERGLUND, L.A. **Recyclable nanocomposite foams of Poly (vinyl alcohol), clay and cellulose nanofibrils – Mechanical properties and flame retardancy**. Composites Science and Technology, 182, 107762. 2019.

MISSOUM, K.; BRAS, J.; BELGACEM, M. N. **Water Redispersible Dried Nanofibrillated Cellulose by Adding Sodium Chloride**. Biomacromolecules, 13, 4118−4125. 2012.

MO, W.; KE, K.; SHEN, X.; LI, B. **The influence of "thermal drying pretreatment" on enzymatic hydrolysis of cellulose and xylan in poplar fibers with high lignin content**. Carbohydrate Polymers, 228, 115400. 2020.

PATRUYO, L. G.; MÜLLER, A. J.; SÁEZ, A. E. **Shear and extensional rheology of solutions of modified hydroxyethyl celluloses and sodium dodecyl sulfate**. Polymer, 43, 6481–6493. 2002.

SILVA, L. E. *et al*. **Cellulose nanofibrils modification with polyaniline aiming at enhancing electrical properties for application in flexible electronics**. Cellulose Chem. Technol., 53 (7-8), 775-786. 2019.

SILVEIRA, R. L.; STOYANOV, S. R.; KOVALENKO, A.; SKAF, M. S. **Cellulose aggregation under hydrothermal pretreatment conditions**. Biomacromolecules, 17, 2582−2590. 2016.

SJÖSTRÖM, E. **Wood chemistry: fundamentals and applications**. Finland: Academic Press, 1981.

THAI, Q. B. *et al*. **Cellulose-based aerogels from sugarcane bagasse for oil spill-cleaning and heat insulation applications**. Carbohydrate Polymers, 228, 115365. 2020.

TOBA, K.; YAMAMOTO, H.; YOSHIDA, M. **Crystallization of cellulose microfibrils in wood cell wall by repeated dry-and-wet treatment, using X-ray diffraction technique**. Cellulose, 20, 633–643. 2013.

TONOLI, G. H. D. *et al*. **Properties of cellulose micro/nanofibers obtained from eucalyptus pulp fiber treated with anaerobic digestate and high shear mixing**. Cellulose, 23, 1239–1256. 2016.

TONOLI, G. H. D. *et al*. **Cellulose micro/nanofibres from Eucalyptus kraft pulp: Preparation and properties**. Carbohydrate Polymers, 89, 80– 88. 2012.

WANG, L.; SANDERS, J. E.; GARDNER, D. G.; HAN, Y. **In-situ modification of cellulose nanofibrils by organosilanes during spray drying**. Industrial Crops and Products, 93, 129-135. 2016.

WANG, Q. *et al*. **Processing nanocellulose to bulk materials: a review**. Cellulose, 26, 7585–7617. 2019.

WERTZ, J.; BÉDUÉ, O.; MERCIER, J. P. **Cellulose science and technology**. Switzerland: EPFL Press, 2010.

XU, F.; SHI, Y.; WANG, D. **X-ray scattering studies of lignocellulosic biomass: a review**. Carbohydrate Polymers, 94, 904– 917. 2013.

YAMANE, C. *et al*. **Two different surface properties of regenerated cellulose due to structural anisotropy**. Polymer Journal, 38, 8, 819–826. 2006.

ZHANG, X. *et al*. **Redispersibility of cellulose nanoparticles modified by phenyltrimethoxysilane and its application in stabilizing Pickering emulsions**. J Mater Sci, 54, 11713–11725. 2019.

ZHAO, Y. *et al*. **Cellulose nanofibers from softwood, hardwood, and tunicate: preparation−structure−film performance interrelation**. ACS Appl. Mater. Interfaces, 9, 13508−13519. 2017.

ZOU, W. *et al*. **Transparent Cellulose Nanofibrils Composites with Two-layer Delignified Rotary-cutting Poplar Veneers (0°-layer and 90°-layer) for Light Acquisition of Solar Cell**. Scientific Reports, 10, 1947. 2020.

**PART II – FIRST MANUSCRIPT (submitted to Carbohydrate Polymers Journal)**

# REDISPERSION AND STRUCTURAL CHANGE EVALUATION OF DRIED MICROFIBRILLATED CELLULOSE

Luiz Eduardo Silva[a], Allan de Amorim dos Santos[b], Lennard Torres[c], Zach McAffrey[c], Artur Klamczynski[c], Greggory Glenn[c], Alfredo Rodrigues de Sena Neto[d], Delilah Wood[c], Tina Williams[c], William Orts[c], Renato Augusto Pereira Damásio[e], Gustavo Henrique Denzin Tonoli[b]

[a] *Forest Science Dept., Federal University of Lavras, P.O. Box 3037, 37200-000, Lavras/MG, Brazil;* lesilvaflorestal@gmail.com

[b] *Forest Science Dept., Federal University of Lavras, P.O. Box 3037, 37200-000, Lavras/MG, Brazil;*

[c] *Bioproducts Research Unit, WRRC, ARS-USDA, Albany, CA 94710, USA*

[d] *Engineering Dept., Federal University of Lavras, P.O. Box 3037, 37200-000, Lavras/MG, Brazil;*

[e] *Research Dept., Klabin S.A., 84275-000, Telemaco Borba/PR, Brazil*

## ABSTRACT

Drying of microfibrillated cellulose (MFC) has always been a challenge for its commercialization, mainly due to its aggregation behavior. In this study, MFC samples were submitted to drying/redispersion cycles at different temperatures. Morphology, crystallinity and mechanical performance of films were analyzed throughout the cycles. Microscopy images, particle size and stability in water showed that aggregation happens more harshly with 5 drying/redispersion cycles and at drying temperatures of 75 and 100°C. Particles once-dried at 20°C presented the same size as MFC-control, forming a web-like structure. Crystallinity and crystallite sizes increased with drying/redispersion cycles especially when dried at 75 and 100°C, however it was not enough to prevent mechanical loss of the films due to aggregation. While oven-drying is not the most suitable method, milder action at room temperature once-drying led to suspension stability in water, morphology and mechanical properties close to never-dried MFC, which makes this treatment a feasible option to maintain cellulose quality.

**Keywords**: cellulose nanofibers, nanofibrils, nanocellulose, hornification, crystallinity, aggregates

# **1** INTRODUCTION

Environmental-friendly materials are searched nowadays to be used as reinforcement or thin films, and it is a constant subject in many researches (Ballesteros et al., 2017; Sena Neto et al., 2015; Liu et al., 2014). Microfibrillated cellulose (MFC) is a nanoscale material with high surface area, due to its many individual nanofibrils (Ioelovich, 2008) that helps binding with matrices and other polymers (Guimarães Júnior et al. 2018; Claro et al., 2018). However, because of cellulose strong hydrogen bonding among chains, causing aggregates, drying is still a setback for MFC handling (Peng, Gardner & Han, 2012). Irreversible or partially irreversible aggregation is frequently reported during drying of cellulose-based materials (Luo et al., 2018; Ballesteros et al., 2017).

The irreversible aggregation of cellulose fibers is caused by intermolecular bonding due to increasing proximity of cellulose chains during drying and is referred to as hornification, usually leading to higher crystallinity and therefore stronger fibers (García-Iruela et al., 2019; Ballesteros et al., 2017; Zimmerman et al., 2016). Even though the process can be favorable to cellulose fibers (Ballesteros et al., 2017), it does not have the same effect on MFC, causing aggregation and fibrillation loss, which motivates studies on proper MFC drying and its effects (Fergunson et al., 2016; Bech; Missoum, Bras & Belgacem, 2012). Then, MFC reinforcement potential becomes limited because of aggregation of the micro/nanofibrils. Avoiding these irreversible processes, MFC must be used without drying (Guimarães Júnior et al., 2018), dispersed in water, or with strong solvents that may cause some changes in cellulose structure (Fergunson et al., 2016) or having salts added prior to drying (Phan-Xuan et al., 2016; Missoum et al., 2012). Usually, chemical modification (Butchosa & Zhou, 2014) or salt addition (Missoum et al., 2012) has been the main focus as strategies to redisperse cellulose nanomaterials. There have been researches on suitable drying method (Peng et al., 2012), drying cycles (Marcin et al., 2014), or drying temperature (Ghasemi et al., 2017), however the drying technologies for MFC films production still deserves investigation on structural changes of cellulose caused by drying methods and drying conditions.

Oven-drying is the cheapest method to be used in large scale drying; however, MFC aggregation is a considerable phenomenon when compared to other methods, like freeze-drying or spray-drying (Zimmermann et al., 2016; Peng et al., 2012). Nonetheless, oven-drying is still the simplest and cheapest, making it a great option to scale up the production, if the aggregation phenomenon could be solved, and understanding controlled drying is the main key to it.

The objective of the present study was to evaluate the effect of number of drying/redispersion cycles (1, 3 and 5 cycles) and drying temperature (20, 50, 75 and 100°C) on morphological, dispersion, mechanical and structural properties of MFC.

## 2 EXPERIMENTAL

### 2.1 Materials

As source of fiber, Klabin S.A. (Paraná/Brazil) donated once-dried bleached Kraft pulps from *Eucalyptus* sp. The starting bleached pulp presented average fibers with around 0.7 mm in length and around 16.0 µm in diameter.

### 2.2 Methods

#### *2.2.1 Pulp fibrillation*

Once-dried bleached pulp was soaked in distilled water (2 wt%) for 48 h, in order to maximize fiber swelling. Afterwards, the dispersion was mixed at 750 rpm for 10 min every 24 h and immediately before fibrillation to individualize the fibers to easy the fibrillation process. A Super Masscolloider Masuko Sangyo - MKCA6-3 model (Japan) grinder was used to mechanically produce MFC. The fibrillation was performed by 5 passages through the grinder at 1,500 rpm with electric current kept between 4 and 6 A, following previous studies (Viana, Potulski, Muniz, Andrade, and Silva, 2018; Fonseca et al., 2016).

#### *2.2.2 Drying/redispersion cycles*

Four different oven-drying temperatures (20, 50, 75 and 100°C) were used as well as five drying/redispersion cycles to each temperature. Even though five drying/redispersion cycles were performed, only the first (C1), third (C3) and fifth (C5) cycles were analyzed, as they were the most representative. In order to assess room temperature (20°C), the samples were dried at constant temperature (around 20°C) and relative humidity (RH) between 30% and 40% for 48 h. A gas-fired batch roaster/dryer from Proctor & Schwartz was used to dry the samples at 50, 75 and 100°C with air circulation and 5% RH, for 8 h each, to ensure complete drying. All samples were dried until constant weight.

Before redispersion, each sample was soaked in distilled water (1 wt%) for 15 h. The dispersion process was performed in a Silverson L5M-A high shear lab mixer in three steps with around 1.3 L each time. The first step was to de-clump the dried fibers sheets, so the general-purpose disintegrating head was used with the mixer operating at 4,500 rpm. Afterwards, the slotted disintegrating head was used at the same rate (4,500 rpm) but due to its

different geometry, the shear is increased and helps to individualize MFC. Finally, an emulsor screen head was used at 7,500 rpm to homogenize the dispersion and further disperse it. Each step lasted 10 min. A portion of never-dried MFC has been used as control (MFC-control).

## 2.3 Characterization

### *2.3.1 Sedimentation of the suspensions*

Sedimentation of the suspension samples was conducted according to Guimarães Júnior et al. (2015). The suspensions were diluted to 0.25 wt% and 15 mL was placed in test tubes for image acquisition. Images were acquired hourly for 8 h. Image analyzer FIJI (Schindelin et al., 2012) was used to estimate MFC decantation in the suspensions, and then stability were calculated according to Eq 1.

$$Stability = \left(\frac{Dispersed}{Total}\right) x\ 100 \quad (1)$$

Where *Dispersed* is the height corresponding to suspended particles, and *Total* is the height of all the liquid in the vessel.

### *2.3.2 Light and scanning electron microscopies of the suspensions*

Aggregates morphology were analyzed with a Leica DM4000B compound light optical microscope (LM). Because the range of light microscope can only reach as low as a few microns, it is not suitable to assess fibrils in nanoscale. However, it is the easiest and quickest way to visualize MFC in its aggregate form. Samples were diluted to 0.1 wt% and stained with aqueous solution of safranin (0.5% v/v) in order to increase the contrast of visible fiber pieces and aggregates. MFC morphology was analyzed in a JEOLJSM-7900F Field Emission Scanning Electron Microscope (FESEM). Prior to imaging, film samples were cast and air-dried for 48 h, then kept at room conditions (RH = 50%, 20°C) to stabilize moisture content. Samples were imaged in film form and specimen stubs with carbon tapes were used to mount the samples. The films were coated with platinum in a Denton (Moorestown, NJ) Desk II sputter coater for 60 s at 100 mTorr vacuum to enhance disperse scattered electrons and produce high-resolution images. The microscope was set to operate at 2.0 kV and 10 µÅ. To better visualize the surface, Z was set to 20 mm, yielding a working distance between 21.0 and 21.4 mm, which was enough to visualize MFC diameters below 1 µm.

*2.3.3 Particle size analysis of aggregates*

The diameter of suspension aggregates was investigated using a laser scattering particle size distribution analyzer (Horiba LA-960) operating in wet mode. For the refraction index of cellulose dispersed in water it was used the value of 1.33 (Huan et al., 2017). 10 runs were made for each treatment. After blanking, each run consisted of agitation, circulation and de-bubbling the water before pouring the dispersion. Then, MFC dispersion was added until transmittance reached values between 85% and 95%, and results are presented as averages of median sizes.

*2.3.4 X-ray diffraction*

Cellulose structure has been analyzed by X-ray diffraction (XRD). XRD patterns were obtained with a X-ray diffractometer (Philips DY971), using CuKα radiation (1.54056 Å) at 45 kV and 40 mA (Tonoli et al., 2016). Scattered rays were gathered in the range of 2θ = 10–40°, at a scan rate of 2°/min. The spectra were acquired from the intact films, attached on the sample holder.

The curves had the noise removed by the adjacent average method with 10 points per window producing smoothed out patterns without losing any peak information. Then, the patterns were deconvoluted with the software Magic Plot (Pro version 2.9) using peak information from French (2014).

For amorphous phase, the peak was set to 2θ=18° and full width at half maximum (FWHM) to 9, only varying its intensity, as suggested in literature (French, 2020; Correia et al., 2016). After deconvolution, crystalline fraction was calculated based on Eq. (2).

$$CF\ (\%) = \frac{A_C}{A_T}\ x\ 100 \qquad (2)$$

Where *CF* is the crystalline fraction, $A_C$ is the sum of the crystalline peaks areas and $A_T$ is the total area of the pattern. Crystallite size of the (200) plane peak was calculated according to Scherrer's equation (Eq. 3).

$$D = \frac{K\ .\lambda}{\beta\ .cos\theta} \qquad (3)$$

Where $D$ is crystallite size (Å), $K$ (0.9) is a constant that refers to crystal shape, $\lambda$ is the wavelength of the ray used (Copper), $\beta$ is the FWHM of the peak, in radians, and $\theta$ is the Bragg's angle of (200) plane diffraction.

*2.3.5 Mechanical properties of MFC films*

The suspension samples were casted to produce films with thickness from 30 to 50 µm and were acclimated at constant relative humidity (50%) for 48 h prior to testing following ASTM D882-12 standard (ASTM, 2012). Tensile tests were performed on dogbone-cut specimens (5 mm cross-section width) using a universal testing machine (Instron, Model 4500, Canton, MA), equipped with 1 kN load cell. Tensile strength and elongation at break were taken from the stress versus strain curves, while Young's modulus was calculated. The tests were performed at a deformation rate of 1 mm/min. Each sample provided 10 specimens for the tensile tests.

*2.3.6 Statistical analysis*

Quantitative analyses that required repetition were submitted to statistical validation. The present work is organized in a factorial design with two independent factors (drying temperature and number of drying/redispersion cycles) and a control sample (MFC-control). Dunnett's test, at 95% significance, was first applied to investigate if the averages were statistically different from the control sample. Secondly, a two-factor analysis of variance (ANOVA) with replication was conducted, also at 95% of significance. This time, F test was applied to verify if there were difference among each factor, as well as interaction among them. Afterwards, in the case of significant interaction between factors, Tukey test has been applied for each treatment to assess the difference among treatments. However, in case of no interaction, Tukey test was used on averages of each factor and helped differentiate results for factors.

## 3 RESULTS AND DISCUSSION

### 3.1 Sedimentation and visual inspection of suspensions

Sedimentation analysis of the suspensions is shown in Figure 1. Because of correlation between particle size, presence of aggregates, and stability, sedimentation analysis has been widely used to assess MFC quality (Guimarães Júnior et al., 2015; Butchosa & Zhou, 2014).

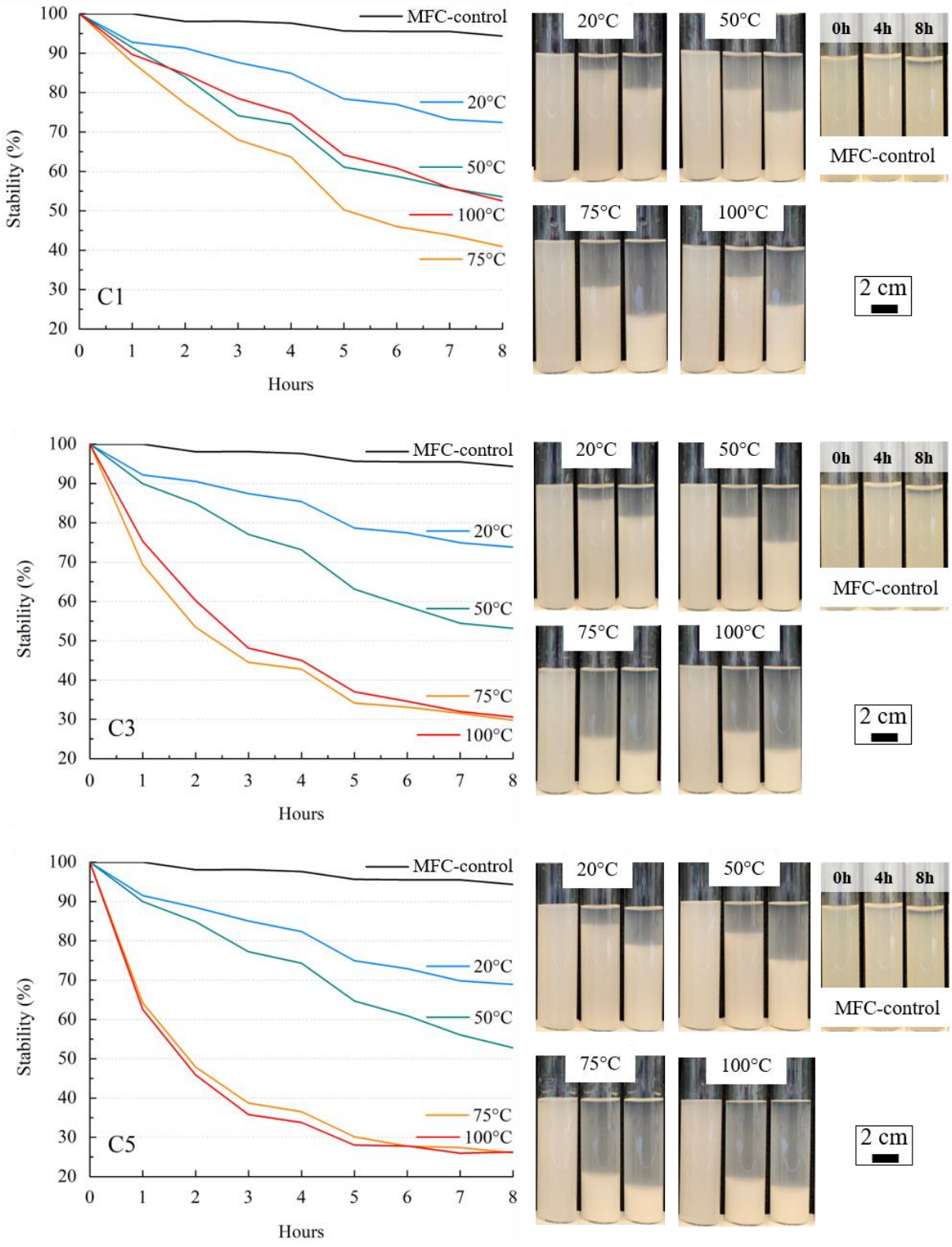


Figure 1: Effect of each drying/redispersion cycle (C1=1cycle, C3=3cycles and C5=5cycles) and drying temperatures (20, 50, 75 and 100°C) on MFC stability in water. MFC-control is presented in the right side of the figure.

Sedimentation results show a clear tendency related to drying/redispersion cycles and higher temperatures (75 and 100°C). However, for 20 and 50°C dried samples, almost no change in stability can be observed, after multiple cycles. Aggregates were formed during drying, and could compromise dispersion stability. Particles in nanoscale dimensions are stable due to Brownian motion, which keeps the particles in suspension caused by the interaction of repelling forces (Fukuzumi et al., 2014). Brownian motion tends to randomize the orientation of fibrils when the dispersion is diluted enough, which keeps them dispersed. On the first cycle (C1), 75 and 100°C samples present stability close to 50°C sample, having a small variation in value due to experimental error. However, this stability is compromised in the following cycles (C3 and C5), making one cycle (C1) the best option, regardless of temperature.

When drying, concentration rises, enhancing interaction and causing it to aggregate or form a network-like structure (Hubbe et al., 2017) caused by both hydrophilic and hydrophobic interactions (Silveira et al., 2016) (Figure 2). Each cycle creates and increases the agglomeration of the cellulose chains and fibrils and consequently the density of already formed aggregates, that sediment more easily, as seen in C3 and C5 (Figure 1), with harsher impact on higher temperatures (75 and 100°C) that has significantly lost stability in water. At room temperature (~20°C), hydrophilic bonds among crystals are what keep the crystallographic structures stable. However, with increasing temperature, hydrophilic bonds increase its stability while hydrophobic bonds become the most stable (Silveira et al., 2016), which eases the aggregation phenomenon, preventing redispersion. Each aggregate that is not redispersed becomes a nucleation site to produce denser aggregates on next cycle (Figure 2).

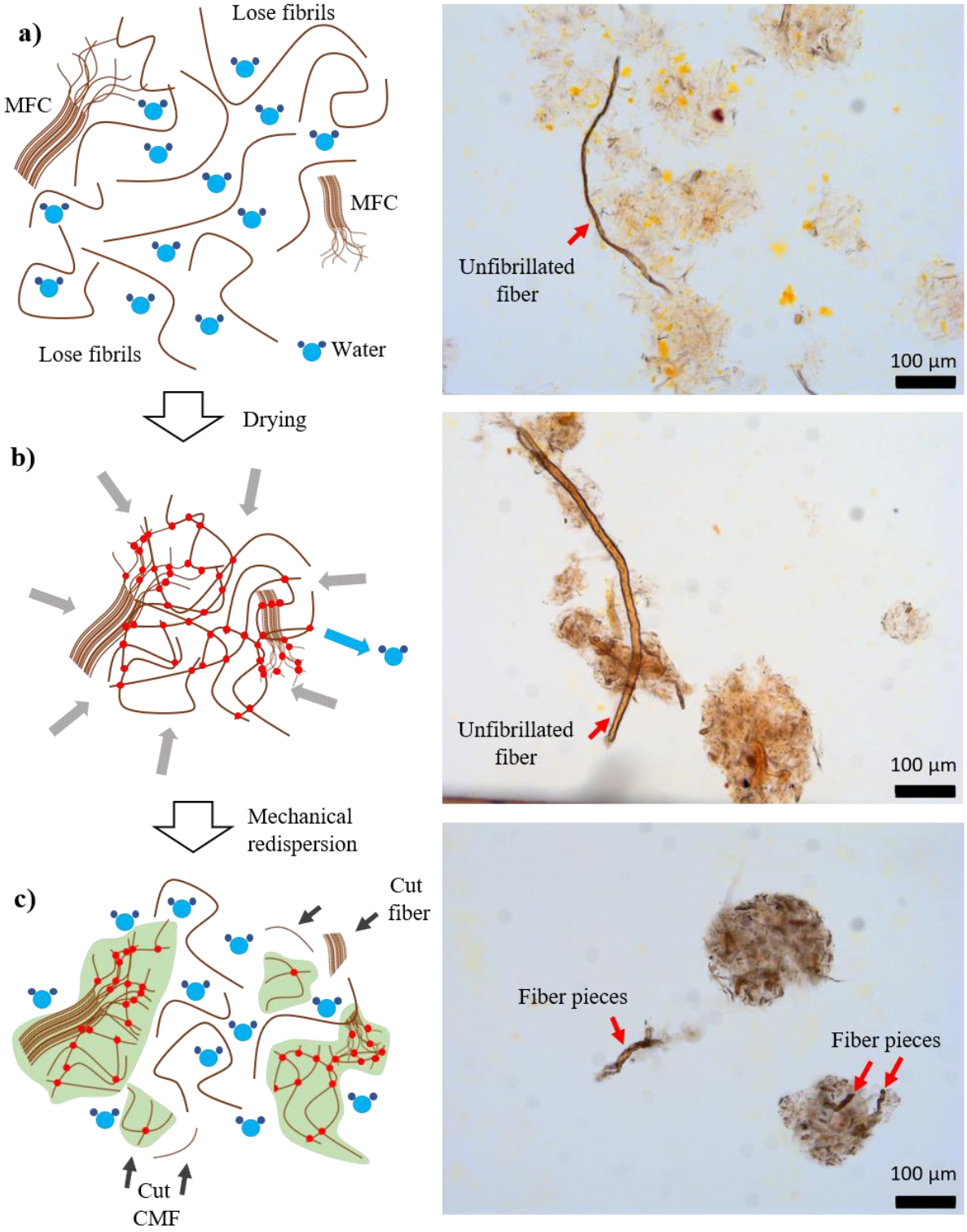


Figure 2: Scheme and light microscopy of drying/redispersion cycles and its impact on aggregates formation: a) MFC and lose fibrils dispersed in water; b) MFC collapsing during water removal; and c) cutting of CMF and residual fiber pieces during mechanical redispersion (black arrows) and aggregates formation (green areas). Red arrows in light microscopy images indicate unfibrillated fibers and residual fiber pieces, after redispersion.

### 3.2 Morphology of the samples by light and electron microscopies

Figure 3 presents the MFC morphology under light and electron microscopes. MFC-control shows that micro/nanofibrils are considerably spread out and have fewer points of contact when dispersed (Figure 3-a) compared to other treatments, but enough to form a net-like structure due to entanglement (Pääkkö et al., 2007). Some fiber pieces can be seen dispersed among the MFC (Arrow 1, Figure 3) and are commonly observed in mechanical treatments (Tonoli et al., 2016; Guimarães Júnior et al., 2015). These residual fiber pieces are secondary cell wall layer (henceforth, fiber pieces) that remained unraveled during the fibrillation process. After a drying/redispersion cycle, fibers may be further fibrillated and MFC cut to smaller pieces caused by prolonged high shear (Benítez & Walther, 2017), forming more compact structures. Fiber pieces in the dispersion help cluster micro/nanofibrils, attracting these smaller pieces to its surface, creating denser aggregates. Even though aggregates seem to become smaller with increasing temperature and number of cycles, the particles are getting denser and more packed due to continuous bonding, as seen by light microscopy (Figure 3) and particle size analysis (Figure 4). This is correlated with the aggregating process and not necessarily with further fibrillation.

Temperature has shown to be as effective as number of drying/redispersion cycles to produce aggregates. Drying of MFC suspensions occurs in three rates (Zimmerman et al., 2016; Peng et al., 2012; Scherer, 1986). Constant drying rate reduces the volume of water and increases the concentration of the suspension. Predominantly, water that is not bound to the fibers, are removed and MFCs move closer together, followed by shrinkage. When the suspension gets concentrated, MFCs have restricted mobility and their surfaces are partially exposed. In this stage, evaporation happens mostly on MFC surface. At this point, MFCs are moving closer as water leaves the system. When the transferring rate of water from inside the suspension to its surface is lower than the rate of water being diffused on the surface, drying enters the second falling rate, and third stage, and it solely happens inside the suspension (Peng et al., 2012). Then, the proximity of fibers is high enough to cause irreversible hydrogen bonding between MFCs, which creates non-dispersible aggregates (Zimmerman et al., 2016). Thus, higher temperatures boost drying rate, which makes MFC easier to collapse and aggregate for samples dried at 75 and 100°C. However, for samples dried at 20°C (Figure 3-e), the rapid drying rate and collapsing reported on the third stage of drying is significantly lowered, producing easier to redisperse and well-spread MFC.

Multiple drying/redispersion cycles have caused the wearing out of MFC with broken nanofibrils and larger empty voids in the films (Figures 4-d and 4-h), creating rougher surfaces. Mechanical treatments during redispersion damages the MFC, making it shorter, collapsing onto aggregates, and, with rapid water removal (such as for drying at 100°C) produces poor distribution of MFC, leaving these voids in the films. The shear produced during the redispersion helps fibers to bend and interlock with each other (Hubbe, 2007) creating "nucleation sites" that could grow into denser aggregates. Falt et al. (2004) correlated higher temperatures, which created higher temperature gradients, with causing rougher surface. This roughness happens by higher surface tension created during drying, which causes surface fibers to bend onto each other due to shrinkage of dried region (Scherer, 1986). Low-temperature drying (20°C) presents smaller drying rates that led to lower surface tension when water is relocated in the suspension. This could explain lower presence of voids, aggregates, and entanglement being formed for samples dried at 20°C, compared to 3 and 5 cycles.

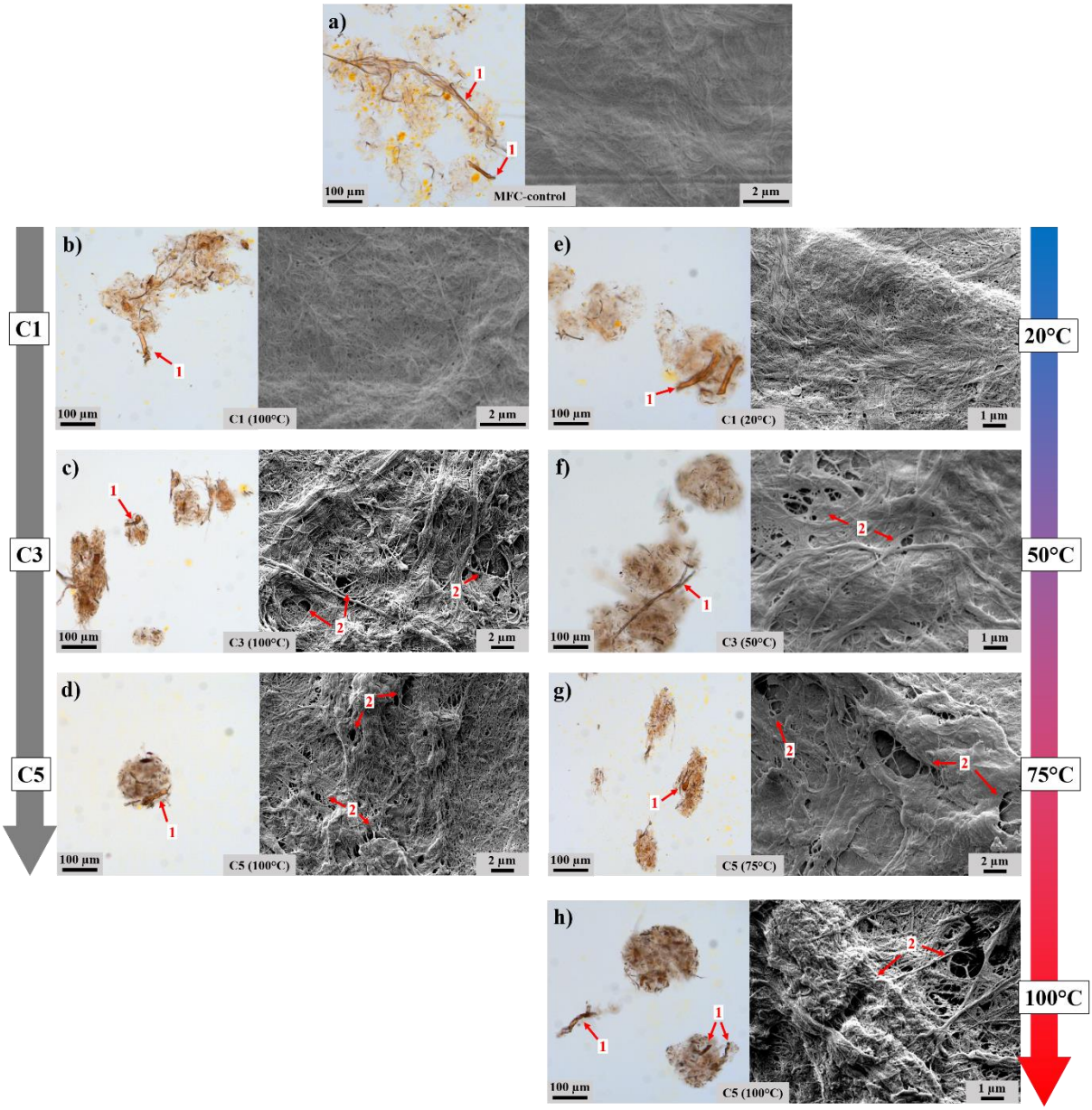


Figure 3: Morphology of the samples seen by light and scanning electron microscopies dried at multiple drying/redispersion cycles and temperatures. a) Never-dried MFC samples (MFC-Control); b-d) differences on morphology caused by increasing the number of drying/redispersion cycles (C1, C3 and C5); e-h) differences on morphology caused by increasing drying temperature (20, 50, 75 and 100°C). Arrow 1: remaining pieces of fibers, promoting nucleation sites; Arrow 2: voids showing the roughness of the sample caused by high drying rates.

### 3.3 Particle size analysis of the suspensions

The easier way to analyze a particle (aggregates, in this case) via light scattering is to correlate its shape to an equivalent sphere, represented by a single number: its diameter (Rawle,

2003). While analyzing the particles, the equipment can generate an arithmetic mean (based on the number of particles per size class) or a moment mean (based on the volume per size class). Keeping in mind that the size distribution is based on a frequency distribution, depending on which parameter it is chosen to base the mean, the result may vary. For instance, if 90% of the total volume is related to 1% of the particles, if we base the mean on volume the result is going to be much higher than if based on number of particles, which would be "diluted" among all particles. Even though both calculations are correct, the results are naturally different because of the calculation applied.

In the present work, measurements were conducted in relation to volume and number of particles (Figures 4-a and 4-b). The results based on number of particles can be thrown down by the presence of either dispersed small nanofibrils or fiber pieces and fibrils that were cut during the redispersion process (Figure 2-c). That way, there are two types of particles in these samples. First, MFC is capable of interlock fibers to form a bigger enough net (Pääkkö et al., 2007) to present sizes even greater than the aggregates. The entanglement, not aggregation, of individualized MFC is the main reason why mechanical strength is enhanced (Butchosa & Zhou, 2014; Pääkkö et al., 2007). The second way is related to the actual size of a particle, in this case, aggregates. Light scattering techniques does not differentiate between those two.

MFC-control presents larger particles compared to dried treatments by both number (8.1±0.1 µm) and volume (53.4±5.8µm) of particles. With the same amount of MFC, the formation of net-like structures requires a greater volume, because of its spread-out feature, generating lighter structures. MFC-Control has more particles with higher volume (number-based), as well as a higher total volume (volume-based), when compared to the dried samples. Regarding the dried samples, the median size at 20°C (number = 8.1±0.1µm, volume = 39.1±6.1µm), are higher than the other temperatures and does not differ from MFC-control calculated by number (using Dunnett's test at 5% significance), showing that it resembles never-dried samples. The disruption of MFC nets, as well as further fibrillation of residual fiber pieces (Arrow 1, Figure 3), which promotes the cutting of fibrils, are what reduces the particle size for dried samples compared to MFC-control. Aggregates start to hinder the formation of larger MFC web structures, that compromises the size of particles dried at 50, 75 and 100°C.

Increasing drying temperature and number of drying/redispersion cycles decreases the capacity of MFC to absorb water (García-Iruela et al., 2019) due to blocking of hydroxyl sites promoted by hornification occurred during drying/redispersion cycles (Marcin et al., 2014). This "blockage" refers to cellulose further bonding caused by aggregation. Silveira et al. (2016) has also shown that with increasing temperature, cellulose becomes more reactive and easier to

form bonds with other chains. Therefore, samples dried at 100°C samples would naturally be the most aggregated.

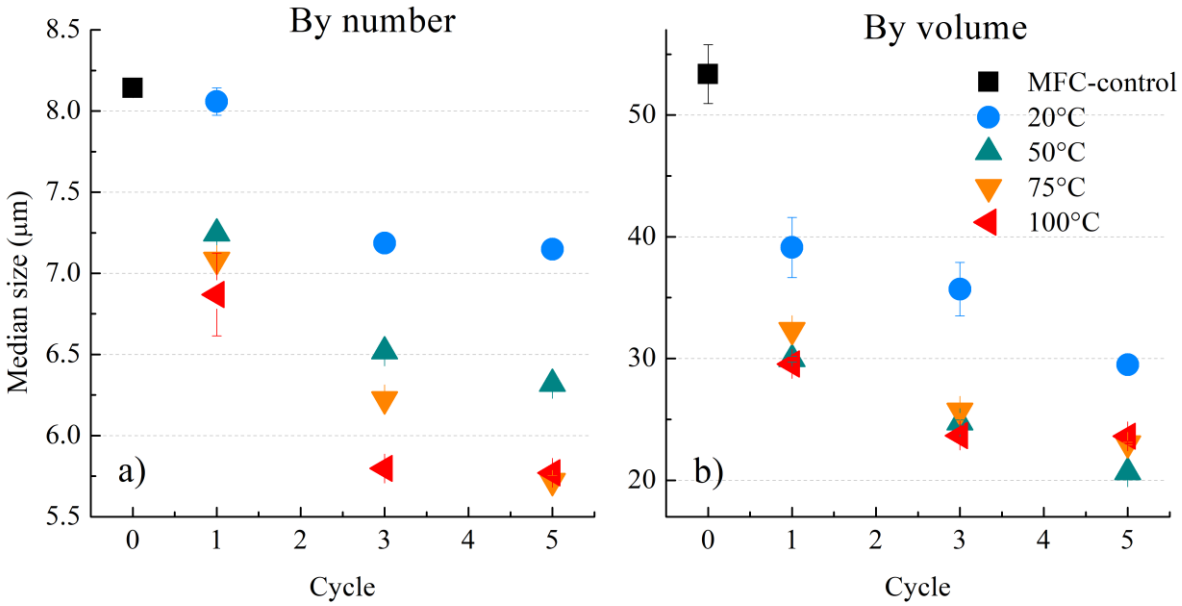


Figure 4: Average particle size values for the different MFC treatments: a) median sizes calculated based on number of particles per size class; b) median sizes calculated based on volume of particles per size class.

### 3.4 X-Ray diffraction

Figure 5 shows the samples diffractograms. There still aren't a consensus about what method to be used on cellulose crystallinity. However, peak deconvolution is more informational and correct than Segal's method, and easier and similar to Rietveld fitting (French, 2020). MFC diffractograms presents the representative peaks of 1β cellulose. The peak around 2θ=21° is related to (200) crystalline plane, while 15° represents the overlap of (1-10) and (110) planes, usually at 2θ=14.8° and 2θ=16.5°, respectively. With increasing crystallinity, these peaks receive less contribution from the amorphous halo, which tends to visually separate them (insets in Figure 5). The small halo close to 2θ=35° is the overlap of multiple small peaks, leaded by (004) crystalline plane (Nam et al., 2016; French, 2014). Even though the amorphous halo masks small peaks close to 2θ=20°, using deconvolution techniques is possible to visualize the pronounced presence of (012) and (102) planes, indicating that the cellulose sample does not have a preferred orientation during the analysis (French, 2014).

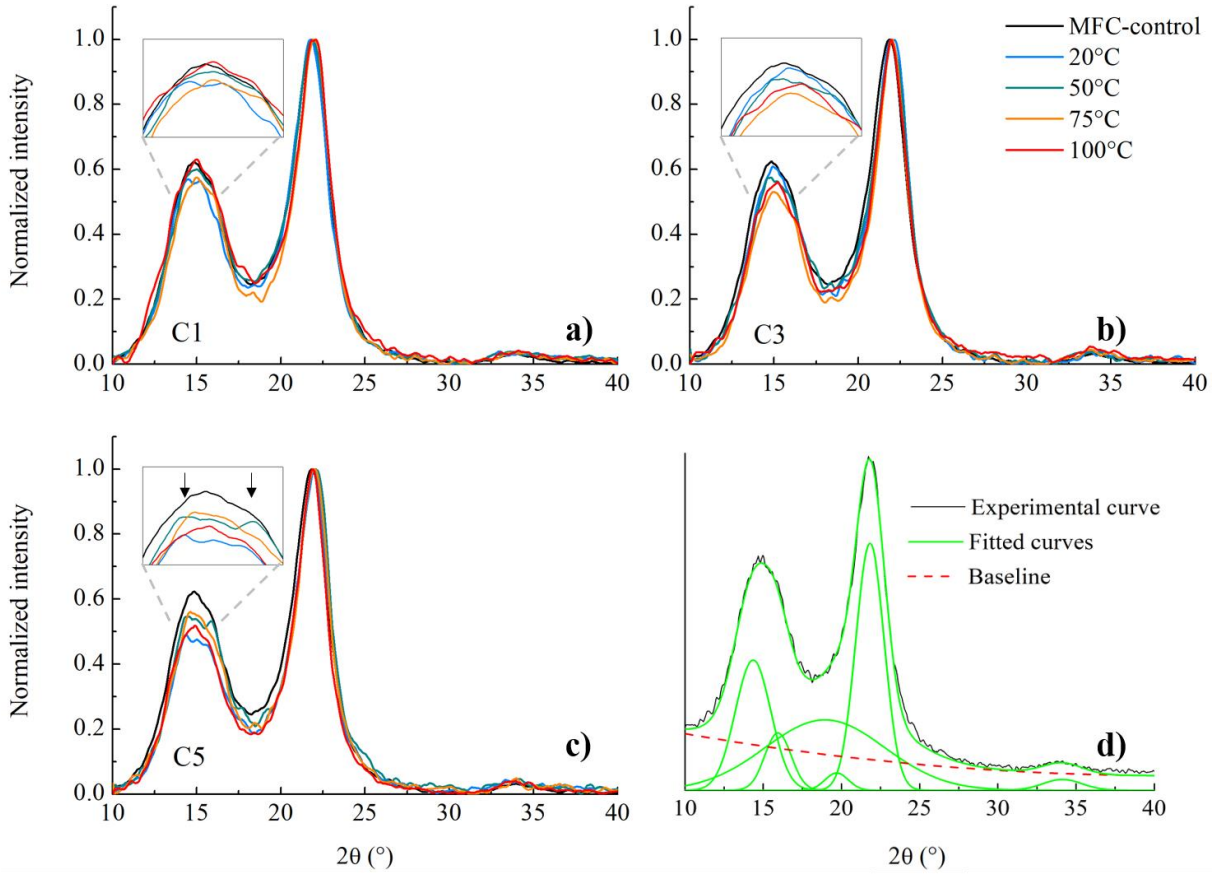


Figure 5: Typical X-ray diffractograms of: (a-c) MFC dried at different temperatures and multiple drying/redispersion cycles (C1=1 cycle; C3=3 cycles; and C5=5 cycles) and different oven-drying temperatures (20, 50, 75 and 100°C); and (d) typical deconvolution used on the diffractograms. Inset images show (1-10) and (110) peaks separation with increasing crystallinity.

Hornification is a well-known factor that causes, especially in higher temperatures, increase in cellulose crystallite size (Mo et al.; 2020; García-Iruela et al.; 2019; Ballesteros et al., 2017). Crystallite size may increase with drying cycles independent of temperature (Toba, Yamamoto and Yoshida, 2013), but increasing drying temperature lead to higher crystallinity (Mo et al., 2020). Mechanical treatments, such as redispersion, may allow reorganization of newly-freed chains onto crystallite surfaces, increasing crystallinity (Ballesteros et al., 2017) (Figure 7-h). Higher temperatures (75 and 100°C) have presented considerably larger crystallites. Hornification at higher temperatures (75 and 100°C) along with the number of drying/redispersion cycles provided increase of crystallinity and crystallite size (Table 1). Less processed samples, such as for 1 cycle at 20°C, presented crystalline profile close to MFC-control, indicating that lower temperatures and less cycling causes less hornification.

Table 1: Crystalline fraction and crystallite size of MFC samples dried at different temperatures (20, 50, 75 and 100°C) and multiple drying/redispersion cycles (C1=1 cycle, C3=3 cycles, C5=5 cycles), as well as MFC-control.

| | | | | | | |
|---|---|---|---|---|---|---|
| Crystalline fraction (%) | MFC-control | | 20°C | 50°C | 75°C | 100°C |
| | 64.9 | C1 | 65.6 | 67.1 | 68.9 | 67.3 |
| | | C3 | 68.5 | 67.4 | 69.2 | 67.3 |
| | | C5 | 69.8 | 68.5 | 69.2 | 68.1 |
| Crystallite size (nm) | MFC-control | | 20°C | 50°C | 75°C | 100°C |
| | 10.7 | C1 | 10.8 | 10.8 | 11.8 | 11.4 |
| | | C3 | 11.1 | 11.4 | 12.5 | 12.2 |
| | | C5 | 11.6 | 11.7 | 12.5 | 12.3 |

### 3.5 Mechanical properties of MFC films

Figure 6 shows the tensile stress-strain curves of the MFC films. Drying/redispersion cycles led to a decrease in mechanical strength of MFC films. Due to mechanical redispersion, is already expected some loss of tensile strength with drying/redispersion cycles, when compared with MFC-control (without drying).

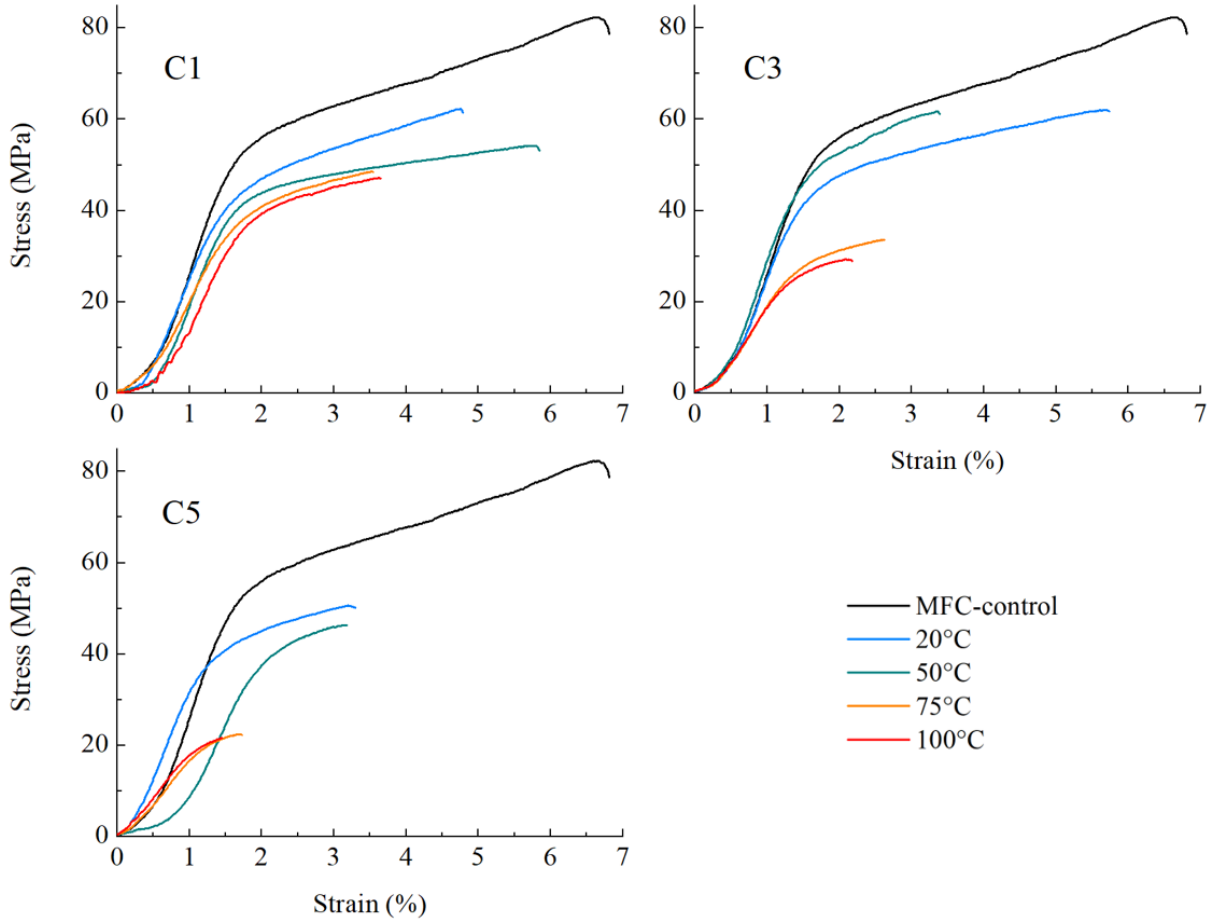


Figure 6: Typical tensile stress-strain curves of MFC-control (without drying) and MFC samples dried at different temperatures (20, 50, 75 and 100°C) and multiple drying/redispersion cycles (C1=1 cycle, C3=3 cycles and C5=5 cycles).

Individualized fibrils have all cellulose chains on their surface to bind with another fibril (Figure 7). When aggregation starts to occur, these binding sites can promote hydrogen bonds with another fibril, or became unreachable, placed in the middle of the aggregate. Only surface fibrils have the possibility to link with any other material. With increasing aggregation, and damage caused on MFC structure by disintegrating nanofibrils, MFC capacity to form tight net-like structures will be lowered, causing mechanical properties of films to progressively drop (Butchosa & Zhou, 2014; Pääkko et al., 2007).

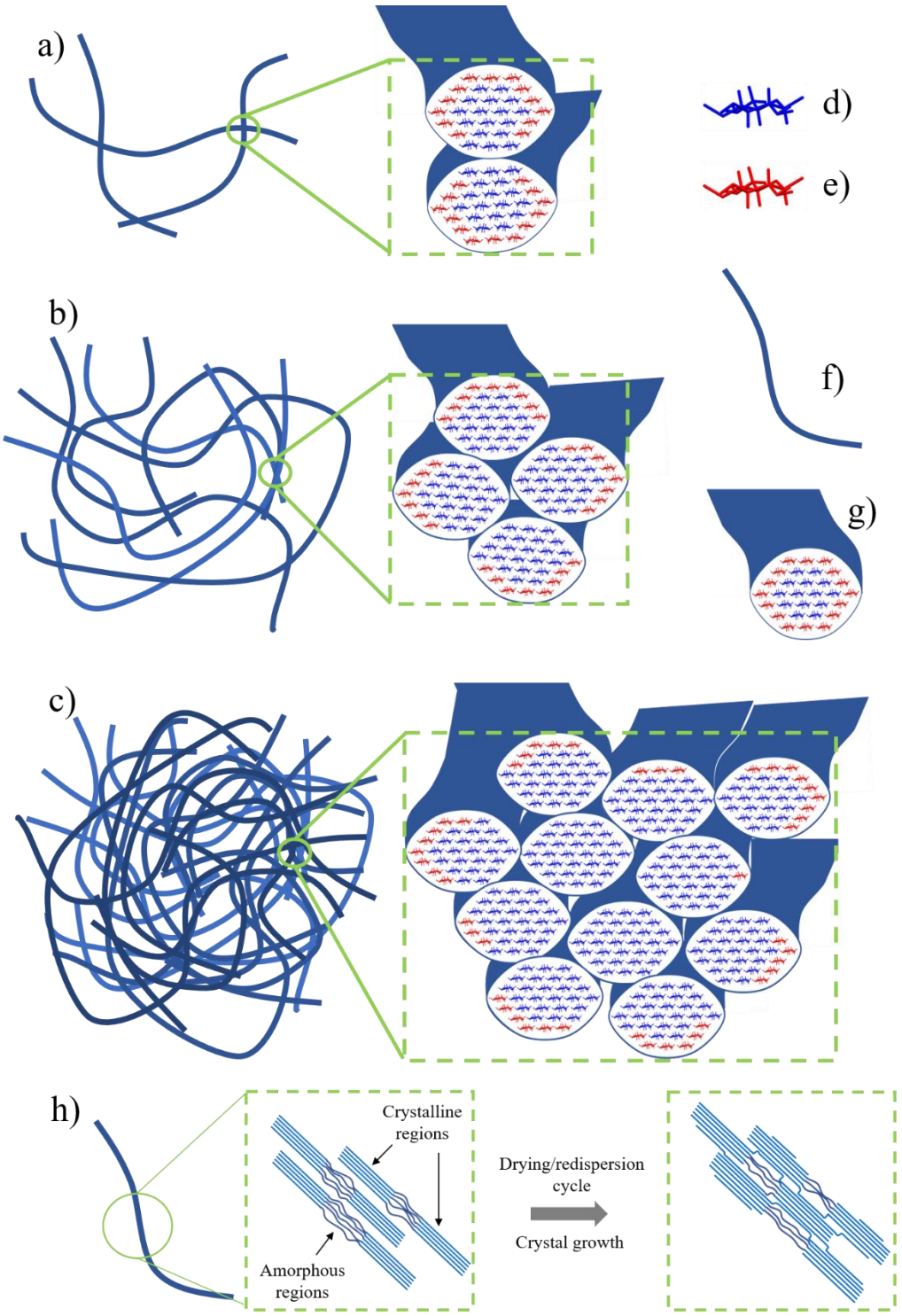


Figure 7: Representation of binding sites dynamic on aggregated MFC: a) secondary bonds between two MFC; b) pilling up of MFC; c) cross-section of a fibril aggregate; d) blue cellulose chains representing already bound or unreachable sites; e) red cellulose chains representing available regions that could be linked to another nearby fibril; f) individualized MFC; g) cross-section of an individualized MFC; h) schematic of cellulose crystallite growth caused by drying/redispersion.

A direct correlation can be seen (Table 2 and 3), that higher temperatures and number of cycles led to lower tensile strength and elongation, caused by increase of number of aggregates, showed in previous analyses. Even though, tensile strength and Young's modulus for samples dried at 20°C were the closest to MFC-control values, elongation was the only property that did not statistically differ from it. However, no other drying treatment has kept MFC film properties during drying/redispersion cycles, even 20°C samples.

Table 2 shows Young's modulus and tensile strength, that were affected by the interaction of temperature and number of cycles applied to each treatment. Lower drying temperatures (20 and 50°C) led to higher film strength than higher temperatures (75 and 100°C), caused by the aggregation process hindering intermolecular bonding throughout the film and not forming the net-like structure that would endure the applied load. Between drying temperatures of 75 and 100°C, tensile strength and stiffness of films were not statistically different, as well, which arises from the same aggregation behavior discussed.

Table 2: Average and standard deviation values of Young's modulus and tensile strength of MFC film samples tested under tensile, showing significant interaction between drying temperature and number of drying/redispersion cycles.

| Young's modulus (GPa) | MFC-control | | 20°C | 50°C | 75°C | 100°C |
|---|---|---|---|---|---|---|
| | 5.8±0.7 | C1 | 4.3±0.3$^{aA}$ | 4.3±0.4$^{aA}$ | 3.5±0.4$^{bA}$ | 3.3±0.3$^{bA}$ |
| | | C3 | 3.8±0.5$^{aAB}$ | 4.3±0.5$^{bA}$ | 2.7±0.2$^{cB}$ | 2.6±0.1$^{cB}$ |
| | | C5 | 3.6±0.8$^{aB}$ | 3.7±0.4$^{aB}$ | 2.0±0.1$^{bC}$ | 2.0±0.2$^{bC}$ |

| Tensile strength (MPa) | MFC-control | | 20°C | 50°C | 75°C | 100°C |
|---|---|---|---|---|---|---|
| | 89.1±14.9 | C1 | 62.4±4.4$^{aA}$ | 56.3±7.0$^{aA}$ | 49.0±6.0$^{bA}$ | 45.5±4.2$^{bA}$ |
| | | C3 | 58.3±3.8$^{aA}$ | 58.1±8.4$^{aB}$ | 33.1±1.3$^{bB}$ | 29.6±1.9$^{bB}$ |
| | | C5 | 49.7±6.8$^{aB}$ | 46.9±4.1$^{aB}$ | 22.4±1.4$^{bC}$ | 21.3±1.2$^{bC}$ |

All combinations of temperature and cycles are significantly different ($p<0.05$) from MFC at Dunnett's test. Within the same line, averages followed by different capital letters are significantly different ($p<0.05$) at Tukey test. Values in the same column followed by different lowercase letters show significant difference ($p<0.05$) at Tukey test.

Elongation at break was not impacted by the interaction of temperature and number of drying/redispersion cycles, as shown in the factorial analysis (Table 3). Even without interaction, both temperatures and number of cycles present a clear tendency. Elongation has a direct correlation with the inter chain bonding of cellulose (Benitez et al., 2013). Here, the mechanical properties of films dried at 100°C experienced 30 to 70% reduction, when compared to MFC-control.

Table 3: Average and standard deviation values for elongation under tensile test for MFC samples submitted to different drying/redispersion cycles (C1=1 cycles, C3=3 cycles, and C5=5 cycles) at different drying temperatures (20, 50, 75 and 100°C), showing no significant interaction between drying temperature and number of cycles.

| | MFC-control | | 20°C | 50°C | 75°C | 100°C | Average |
|---|---|---|---|---|---|---|---|
| Elongation (%) | | C1 | 5.9±1.2* | 5.0±0.8 | 3.5±0.8 | 3.9±0.7 | **4.6±1.3$^{A}$** |
| | **6.1±1.8*** | C3 | 5.0±0.7 | 3.1±0.8 | 2.6±0.2 | 2.2±0.3 | **3.2±1.2$^{B}$** |
| | | C5 | 3.6±0.8 | 2.9±0.6 | 1.8±0.4 | 1.6±0.1 | **2.5±1.0$^{C}$** |
| | | Average | **4.8±1.3$^{a}$** | **3.7±1.2$^{b}$** | **2.6±0.9$^{c}$** | **2.6±1.1$^{c}$** | |

* Value significantly different ($p<0.05$) from MFC at Dunnett test.
Values followed by different capital letters show significant difference ($p<0.05$) at Tukey test.
Averages followed by different lowercase letters are significantly different ($p<0.05$) at Tukey test.

Usually, higher crystallinity leads to higher tensile strength of fibers (Kim et al., 2017). However, even though cycling and higher temperatures have increased crystallinity of the samples (Table 1), mechanical properties did not follow the same tendency (Tables 2 and 3). In this case, higher crystallinity was not enough to compensate the aggregation process and hindering of MFC network formation upon drying into films.

## 4 CONCLUSIONS

In this study, structural and morphological changes of MFC promoted by drying/redispersion cycles at different temperatures were evaluated. The aggregation process was more intense to higher drying temperatures (75° and 100°C) and higher number of drying/redispersion cycles (5 cycles). Drying temperatures higher than 50°C and higher number of cycles were less successful to form an interconnected net-like structure as occurred in MFC-control (never-dried), caused by the production of aggregates into the film structure. Even though reorganization of amorphous cellulose at higher temperatures led to increase of crystallinity of the cellulose, the aggregates formation has significantly lowered mechanical strength of dried MFC films. MFC that was once-dried at room temperature (20°C) was the only treatment able to maintain properties similar to MFC-control (no drying treatment), which shows that lower temperatures and less cycling is the most suitable way to dry MFC with less hornification of the fibrils and smooth changes on their suspension stability in water and structure (crystalline organization), maintaining mechanical performance of the films, which is an important contribution for development and optimization of drying technologies for MFC films.

## ACKNOWLEDGMENTS

This study was financed in part by the Coordenação de Aperfeiçoamento de Pessoal de Nível Superior – Brasil (CAPES) – Finance Code 001.The authors also acknowledge the support of the Fundação de Amparo à Pesquisa do Estado de Minas Gerais – FAPEMIG, Conselho Nacional de Desenvolvimento Científico e Tecnológico – CNPq, and the Bioproducts Research Unit (BRU - ARS) at the United States Department of Agriculture (Albany - CA).

## REFERENCES

ASTMD 882-12, (2012). Standard test method for tensile properties in thin plastic sheeting, *ASTM International*, West Conshohocken, PA.

Ballesteros, J. E. M., et al. (2017). Potential of the hornification treatment on eucalyptus and pine fibers for fiber-cement applications. *Cellulose*, *24*, 2275-2286.

Benítez, A. J., & Walther, A. (2017). Cellulose nanofibril nanopapers and bioinspired nanocomposites: a review to understand themechanical property space. *Journal of Materials Chemistry A, 5*, 16003-16024.

Butchosa, N., & Zhou, Q. (2014). Water redispersible cellulose nanofibrils adsorbed with carboxymethyl cellulose. *Cellulose, 21*, 4349–4358.

Claro, P. I. C., et al. (2018). Curaua and eucalyptus nanofibers films by continuous casting: Mechanical and thermal properties. *Carbohydrate Polymers, 181*, 1093–1101.

Correia, V. C., et al. (2016). Grinding process for the production of nanofibrillated cellulose based on unbleached and bleached bamboo organosolv pulp. *Cellulose, 23*, 2971–2987.

Fergunson, A., et al. (2016). Understanding the Dispersion and Assembly of Bacterial Cellulose in Organic Solvents. *Biomacromolecules, 17*, 1845−1853.

Fonseca, A. S., et al. (2016). Micro/nanofibras celulósicas de Eucalyptus em fibrocimentos extrudados. *CERNE, 22*, 59-68.

French, A.D. (2014). Idealized powder diffraction patterns for cellulose polymorphs. *Cellulose, 21*, 885–896.

French, A.D. (2020). Increment in evolution of cellulose crystallinity analysis. *Cellulose, 27*, 5445–5448.

Fukuzumi, H., et al. (2014). Dispersion stability and aggregation behavior of TEMPO-oxidized cellulose nanofibrils in water as a function of salt addition. *Cellulose, 21*, 1553–1559.

García-Iruela, A., et al. (2019). Effect of vacuum/pressure cycles on cell wall composition and structure of poplar wood. *Cellulose, 26*, 8543–8556.

Gardner, D. J., et al. (2008). Adhesion and surface issues in cellulose and nanocellulose. *Journal of Adhesion Science and Technology, 22*, 545–567.

Ghasemi, S., et al. (2017). Dry-Spun Neat Cellulose Nanofibril Filaments: Influence of Drying Temperature and Nanofibril Structure on Filament Properties. *Polymers, 9*, 392.

Guimarães Júnior, M., et al. (2015). Preparation of Cellulose Nanofibrils from Bamboo Pulp by Mechanical Defibrillation for Their Applications in Biodegradable Composites. *Journal of Nanoscience and Nanotechnology, 15*, 1–18.

Guimarães Júnior, M., Teixeira, F. G., & Tonoli, G. H. D. (2018). Effect of the nano-fibrillation of bamboo pulp on the thermal, structural, mechanical and physical properties of nanocomposites based on starch/poly (vinyl alcohol) blend. *Cellulose, 25*, 1823–1849.

Huan, S. et al. (2017). Formulation and composition effects in phase transitions of emulsions costabilized by cellulose nanofibrils and an ionic surfactant. *Biomacromolecules, 18*, 4393−4404.

Hubbe, M. A. (2007). Flocculation and redispersion of cellulosic fibers suspensions: a review of effects of hydrodynamic shear and polyelectrolytes. *BioResources, 2*, 296–331.

Hubbe, M. A., et al. (2017). Rheology of nanocellulose-rich aqueous suspension: a review. *BioResources, 12*, 9556–9661.

Ioelovich, M. (2008). Nanostructured cellulose: Review. *BioResources, 3*, 1403-1418.

Liu, S., et al. (2014). Evolution of cellulose into flexible conductive green electronics: a smart strategy to fabricate sustainable electrodes for supercapacitors. *RSC Advances*, 4, 34134-34143.

Luo, J., et al. (2018). Post-sulfonation of cellulose nanofibrils with a one-step reaction to improvedispersibility. *Carbohydrate Polymers, 181*, 247–255.

Marcin, D., et al. (2014). Influence of number of drying cycles on cellulose fibers hornification process. *Forestry and Wood Technology, 86*, 82-85.

Missoum, K., Bras, J., & Belgacem, M. N. (2012). Water Redispersible Dried Nanofibrillated Cellulose by Adding Sodium Chloride. *Biomacromolecules, 13*, 4118−4125.

Mo, W., et al. (2020). The influence of "thermal drying pretreatment" on enzymatic hydrolysis of cellulose and xylan in poplar fibers with high lignin content. *Carbohydrate Polymers, 228*, 115400.

Pääkkö, M., et al. (2007). Enzymatic hydrolysis combined with mechanical shearing and high-pressure homogenization for nanoscale cellulose fibrils and strong gels. *Biomacromolecules, 8*, 1934-1941.

Peng, Y., Gardner, D. J., & Han, Y. (2012). Drying cellulose nanofibrils: in search of a suitable method. *Cellulose, 19*, 91-102.

Phan-Xuan, T., et al. (2016). Aggregation behavior of aqueous cellulose nanocrystals: the effect of inorganic salts. *Cellulose, 23*, 3653–3663.

Rawle, A. F. (2003). The Basic Principles of Particle Size Analysis. *Surface Coatings International Part A: Coatings Journal, 86*, 58-65.

Scherer, G. W. (1986). Drying gels. *Journal of Non-Crystalline Solids, 87*, 199-225.

Schindelin, J., et al. (2012). Fiji: an open-source platform for biological-image analysis. *Nature methods, 9*, 676-682.

Sena Neto, A. R., et al. (2015). Comparative study of 12 pineapple leaf fiber varieties for use as mechanical reinforcement in polymer composites. *Industrial Crops and Products, 64*, 68–78.

Silveira, R. L., et al. (2016). Cellulose Aggregation under Hydrothermal Pretreatment Conditions. *Biomacromolecules, 17*, 2582−2590.

TAPPI. (1994). Fines fraction of paper stock by wet screening (T 261 cm-94).

Toba, K., Yamamoto, H., & Yoshida, M. (2013). Crystallization of cellulose microfibrils in wood cell wall by repeated dry-and-wet treatment, using X-ray diffraction technique. *Cellulose, 20*, 633–643.

Tonoli, G. H. D., et al. (2016). Properties of cellulose micro/nanofibers obtained from eucalyptus pulp fiber treated with anaerobic digestate and high shear mixing. *Cellulose, 23*, 1239–1256.

Viana, L. C., Potulski, D. C., Muniz, G. I. B., Andrade, A. S., and Silva, E. L. (2018). Nanofibrillated cellulose as an additive for recycled paper. *CERNE, 24*, 140-148.

Zimmermann, M. V. G., et al. (2016). Drying techniques applied to cellulose nanofibers. *Journal of Reinforced Plastics and Composites, 35*, 682–697.

**PART III – SECOND MANUSCRIPT (Formatted according to Carbohydrate Polymers Journal)**

# SODIUM CHLORIDE AND SODIUM DODECYL SULFATE AS ADDITIVES TO ENHANCE DISPERSIBILITY IN CELLULOSE MICRO/NANOFIBRILS

Luiz Eduardo Silva [a], Riley Simson [b], Lennard Torres [c], William Hart-Cooper [c], Cao Trung [c], Artur Klamczynski[c], Greggory Glen [c], Alfredo Rodrigues de Sena Neto [d], Tina Williams [c], Delilah Wood [c], William Orts [c], Gustavo Henrique Denzin Tonoli [b]

[a] *Forest Science Dept., Federal University of Lavras, P.O. Box 3037, 37200-000, Lavras/MG, Brazil;* lesilvaflorestal@gmail.com

[b] *Forest Science Dept., Federal University of Lavras, P.O. Box 3037, 37200-000, Lavras/MG, Brazil;*

[c] *Bioproducts Research Unit, WRRC, ARS-USDA, Albany, CA 94710, USA*

[d] *Engineering Dept., Federal University of Lavras, P.O. Box 3037, 37200-000, Lavras/MG, Brazil;*

## ABSTRACT

Microfibrillated cellulose (MFC) are strong, low-cost, and renewable material. However, during drying, aggregation process can happen, lowering tensile strength and changing MFC morphology. Therefore, the present work aims to evaluate the use of additives that inhibit hydrogen bonding to prevent MFC from clumping during redispersion. TEMPO-mediated oxidation followed by high-shear mixing was used to produce MFC. Four treatments were then produced. Never-dried (ND) MFC, as control, and three dried samples: with only MFC (DR), and with addition of sodium chloride (D-Na) and sodium dodecyl sulfate (D-SD). The effects of the additives on the morphological, water stability, and mechanical behavior of the MFC were investigated. DR presented visible aggregates with lower stability in water (less than 85%) and the least resistant films from all the samples. Even though D-Na has shown particle size similar to D-SD, its tensile strength and strain at break were considerably lower. D-SD presented the most stable dispersion with smaller particles and porous structure with a residual presence of SDS on the washed sample. However, residual SDS has increased in 28% tensile strength and 48% in stiffness for D-SD sample compared to ND. Hence, D-SD was the most suitable method of drying, preserving MFC properties, with enhancement of mechanical properties.

**Keywords**: cellulose nanofibrils, surfactant, aggregates, NaCl, SDS.

# 1 INTRODUCTION

Recently, cellulose-based materials have gained attention due to their low cost, high strength to weight ratio, and biodegradability (Guimaraes Junior, Teixeira and Tonoli, 2018; Tonoli et al., 2016). Microfibrillated cellulose (MFC) is a high-value material with even higher strength when compared with macrofibers (Tonoli et al., 2016) due to its many individual nanofibrils forming a net-like structure (Ioelovich, 2008; Paakko et al., 2007). This is possible because of the high hydrophilicity of cellulose promoted by hydroxyl groups present in its chains (Liu et al., 2014; Gardner et al., 2008). Thus, many researches have risen to understand and apply its properties (Arantes et al., 2019; Guimaraes Junior, Teixeira and Tonoli, 2018; Claro et al., 2018; Ballesteros et al., 2017).

Because of high strength to weight ratio, freeze-drying has been largely used in different applications, such as pharmaceutical, tissue and packaging (Han et al., 2013). Negative molding and ice templating with cellulose micro/nanofibrils are some other uses for the process (Medina, Carosio, and Berglung, 2019; Antonini et al., 2019). However, even though freeze-drying is the most used drying technique for MFC in laboratories (Wang et al., 2019), some aggregates can be formed during lyophilization (Zimmerman et al., 2016; Peng et al., 2012). The aggregation process occurs because of irreversible bonds within cellulose fibrils during drying (Ballesteros et al., 2017; Eyholzer et al., 2010). This inter-fibril bond can be avoided if the hydrogen bonding can be inhibited by another component. Missoum, Bras and Belgacem (2012) have used a salt, NaCl, prior to drying to avoid MFC aggregation. The authors have claimed that a completely redispersible suspension was achieved. However, no further investigation on mechanical strength, for instance, was made.

Another possible solution would be using an ionic surfactant. Sodium dodecyl sulfate is a negatively charged surfactant (Xiang et al., 2018) just like cellulose (Xiang et al., 2018; Huan et al., 2017) that is employed in many common products (Lo et al., 2014). However, under a certain concentration, sodium dodecyl sulfate is temporarily able to crosslink nanofibrils (Patruyo, Müller and sáez, 2002), keeping a 3D network during drying. As of yet, SDS has not yet been used to produce redispersible MFC.

Therefore, the present study aims to evaluate the ability of sodium chloride and sodium dodecyl sulfate in produce redispersible MFC samples. The effects of the additives on the morphological, water stability, and mechanical behavior of the MFC were investigated.

## 2 EXPERIMENTAL

### *2.1 Materials*

As a source of fiber, Klabin S.A (Paraná/Brazil) donated once-dried bleached kraft pulps from Eucalyptus sp. (hardwood). The bleached pulp presented average fibers with 0.7 mm in length and 16 µm in diameter. 2,2,6,6-tetramethylpyperidine-1-oxyl (TEMPO) was purchased from Oakwood Chemical (South Carolina/USA). Sodium chloride, sodium bromide and sodium dodecyl sulfate (SDS) were purchased from Fisher Chemical, Sigma-Aldrich, and J.T. Baker, respectively. All chemicals were used without further purification.

### *2.2 TEMPO-mediated oxidation of fibers*

TEMPO-mediated oxidation of cellulose fibers was carried out according to a method in literature (Saito and Isogai 2004). Cellulose fibers (30 g) were suspended in water (1.5 L) with previously dissolved TEMPO (0.016 g) and sodium bromide (0.1 g) per gram of fiber. After 30 minutes of agitation, 5 mmol/g of sodium hypochlorite (NaClO) solution was added dropwise. While NaClO solution was added, the pH was maintained between 9.5 and 10.5 by using 0.5% NaOH solution. Afterwards, the dispersion was kept under agitation for three hours and 0.5% NaOH solution was again used to keep the pH above 9.5 and below 10.5 and help the carboxylation takes place. When the reaction was finished, 50 mL of ethanol was poured to completely stop the oxidation. Later, the dispersion was strained on a 75-mesh sieve and thoroughly rinsed with distilled water to remove any trace of oxidizing agents.

### *2.3 Pulp fibrillation*

After TEMPO-mediated oxidation, the fibers were resuspended in distilled water to 1 wt% concentration. Then, the dispersion was mixed for 20 minutes (Figure 1) on Silverson L5M-A high shear lab mixer. Two heads were used to maximize fibrillation. The slotted disintegrating head was used first, for 10 minutes, to individualize the fibers and start the fibrillation process. Afterwards, the emulsor screen was selected to further fibrillate and homogenize the dispersion. The final product was a combination of cellulose micro/nanofibrils (MFC).

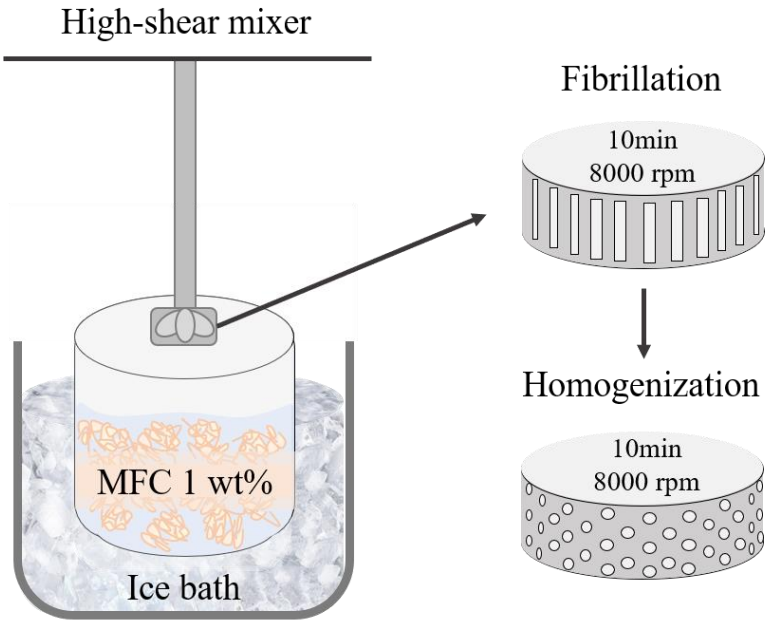


Figure 1: Schematics of high-shear mixing employed on the production of MFC.

*2.4 Freeze-drying the samples*

Three treatments and a control with 500 mL of 1 wt% MFC dispersion each were prepared before freeze-drying (see Table 1).

Table 1: Preparation, concentration and conditions of the samples.

| **Sample ID** | **Additive** | **Concentration added** | **Condition** |
|---|---|---|---|
| ND | X | X | Never-dried MFC |
| DR | X | X | Dried without any additive |
| D-Na | Sodium chloride (NaCl) | 10 mM | Mixed and dried with NaCl |
| D-SD | Sodium dodecyl sulfate (SDS) | 10 mM | Mixed and dried with SDS |

In order to freeze-dry MFC samples, the dispersions were poured into tinfoil molds and then immersed in liquid nitrogen. In a matter of seconds, the samples were frozen solid and taken to a freeze dryer (FreeZone 4.5 Liter Console Freeze Dry Systems – Labconco) under 0.2 mBar vacuum pressure and -54°C for 48 hours to completely dry the samples. When working with salts both pH and concentration can affect aggregation of MFC. On the present study, NaCl was kept bellow critical aggregation concentration for MFC (Phan-Xuan et al., 2016), and used at neutral pH, which combined with the used concentration did not produced a screening effect on MFC (Fall et al., 2011).

*2.5 Redispersion*

After freeze-drying the samples, the specimens were redispersed and filtered on a Britt dynamic drainage jar (Seattle, Washington, United States) following a modified T 261cm-94 (TAPPI, 1994) procedure. In this step, 0.5 g of the sample (dry weight of 500 mL 1 wt% MFC dispersion) was resuspended in 500mL of distilled water and mixed at 1500 rpm for 10 seconds and then the drain was opened slightly. Without completely draining the sample, 500 mL aliquots of distilled water were added until 7 L of water was reached. During the filtration, MFC was redispersed. This procedure was used not only for redispersion but for the removal of NaCl and SDS from the samples. After 2 L washed, the filtrated was below the critical micelle concentration for SDS, exhibiting no visual indication of SDS presence, even considering the effect of MFC in the solution (Tardy et al., 2017; Huan et al. 2017). The last 5 L wash was conducted as a precaution to remove all traces of SDS. To allow any comparison among the samples, all samples was filtered with 7 L of distilled water, including ND.

*2.6 Sedimentation*

The samples stability in water was conducted following Guimaraes et al (2015). Aliquots of 30 mL diluted samples (0.25 wt%) were placed in test tubes on a stable location for the procedure. For the first 8 hours, pictures of the samples were taken. Image analyzer FIJI (Schindelin et al. 2012) was used to measure qualitatively MFC decantation. The stability in water was calculated according to the following equation 1:

$$Stability\ (\%) = \frac{Decanted}{Total}\ x\ 100 \qquad (1)$$

Where *Total* is the height of all the liquid in the tube and *Decanted* is *Total* minus the height of clear water, where fibers are absent.

*2.7 Light Microscopy*

The morphology of the redispersed samples were analyzed with a Leica DM4000B compound light optical microscope (LM) to assess aggregate formation. For this, each treatment had a diluted aliquot (0.1 wt%) stained with aqueous solution of safranin (0.5% v/v) to enhance the contrast of the micro/nanofibrils as well as the aggregates.

*2.8 Scanning Electron Microscopy*

A JEOL JSM-7900F Field Emission Scanning Electron Microscope (FESEM) was used to image the samples and analyze their morphology. Images were taken from the freeze-dried samples before redispersion. In order to prepare the specimens, carbon tape was used on stubs and the samples were placed on top of the tape. To enhance contrast of the images, a platinum coating was applied in a Denton (Moorestown, NJ) Desk II sputter coater for 60s at a 100mTorr vacuum to help disperse scattered electrons. Microscope set up was 2.0 kV and 10 µÅ of voltage and current, respectively. Aiming clearer images at high magnification, Z was set to 20 mm and a working distance between 21.0 and 21.4 mm was used.

*2.9 Particle Size*

Laser scattering particle size distribution analyzer (Horiba LA-960) has been used to quantify aggregates size, operating in wet mode. For all the measurements, cellulose refraction index was set to 1.33, as it was the value corresponded to MFC dispersed in water. Each treatment was analyzed in triplicates. After blanking the analyzer and before each measurement, the same procedure was conducted: agitation, circulation and de-bubbling of the water in vessel attached to the machine. Afterwards, MFC was added until transmittance reached values between 85% and 95%. The results were calculated based on classes of volume and number, and are shown in averages of median size.

*2.10 Fourrier transformed infrared*

The samples were subjected to FTIR-ATR spectroscopy using a Thermo Scientific spectrometer equipped with the Smart iTX accessory, with one reflection diamond slit. The spectra acquisition was obtained in the range from 4000 to 400 $cm^{-1}$, wavenumber, operating in the absorbance mode with 4 $cm^{-1}$ resolution and performing 16 scans per sample.

*2.11 Mechanical Properties*

From each treatment, films were prepared by casting to be analyzed regarding mechanical properties. A universal testing machine (Instron, Model 4500, Canton, MA), equipped with 1 kN load cell was used to perform tensile test on the samples. The test followed ASTM D882-12 standard (ASTM, 2012), and specimens were previously conditioned accordingly. Tensile strength and elongation at break were directly taken from the stress/strain curves, while Young's modulus was calculated by the inclination of the elastic portion. An extension rate of 1 mm/min was used and 10 specimens per sample were analyzed.

# 3 RESULTS

## *3.1 Fibrillation of the fibers*

TEMPO-mediated oxidation followed by high-shear mixing was successful to open fiber cell wall and fibrillate it into MFC. Figure 2 shows, at different magnifications, the MFC making process. Fiber swelling caused by TEMPO-mediated oxidation increases the effectiveness in fibrillation (Saito and Isogai, 2004). While swelling the fiber, oxidation creates weak spots (Figure 2.a) that later are break down into cellulose fibrils (Osong et al., 2016). Mechanical mixing can also detach MFC from the fibers from one end through the whole fiber in a motion similar to “untying a rope” (Figure 2.b). Likewise, in this case, swelling eases the mechanical process by helping water enter the fiber cell wall and weakening inter-fiber hydrogen bonds. This happens due to heterogenous swelling of the fiber, commonly referred as ‘ballooning’, that will swell parts of the fibers and then disrupt the cell wall into MFC (Sim, Alam, Godbout and Ven, 2014; Cuissinat, Navard and Heinze, 2008). After fibrillation, even though some fibers are remaining, MFC was dispersed and formed a fibrils network that was not fully discernible in light microscopy (Figure 2.c), which could enhance mechanical properties of this material.

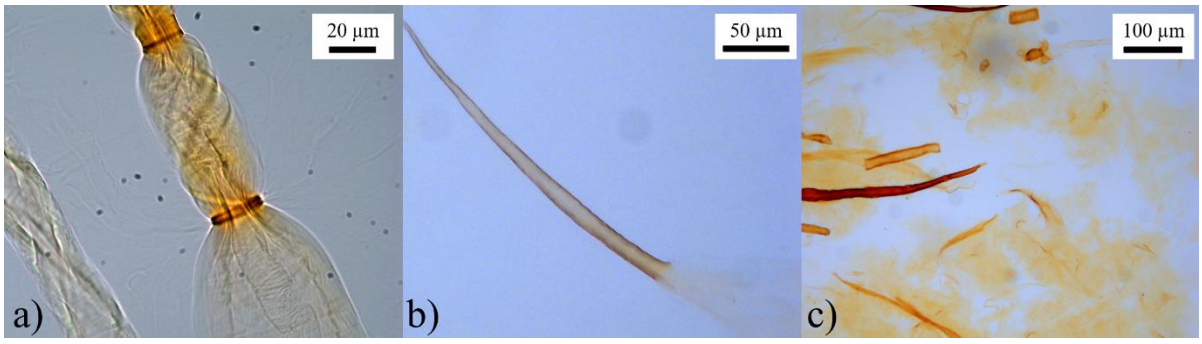


Figure 2: Light microscopy of the morphology of MFC produced by mechanical fibrillation. a) weak spots on cell wall; b) cellulose fiber with a fibrillated end; and c) dispersed MFC.

## *3.2 Sedimentation and visual inspection*

Sedimentation is a qualitative method to verify the success of redispersion of MFC (Zhang et al., 2019; Guimaraes Junior, Teixeira and Tonoli, 2018; Guimaraes Junior et al., 2015). Because of the Brownian motion, nanometric-sized fibers tend to stay afloat caused by repelling forces of nearby fibers (Fukuzumi, Tanaka, Saito and Isogai, 2014). The MFC that clump together to form aggregates are submitted to gravity and pulled down to the bottom of

the vessel. Thus, more stable dispersions would have less precipitate gathering at the bottom of the vessel after certain duration. During the 8 hours that the analysis was performed, no visible precipitation occurred on 'ND' sample (Figure 3).

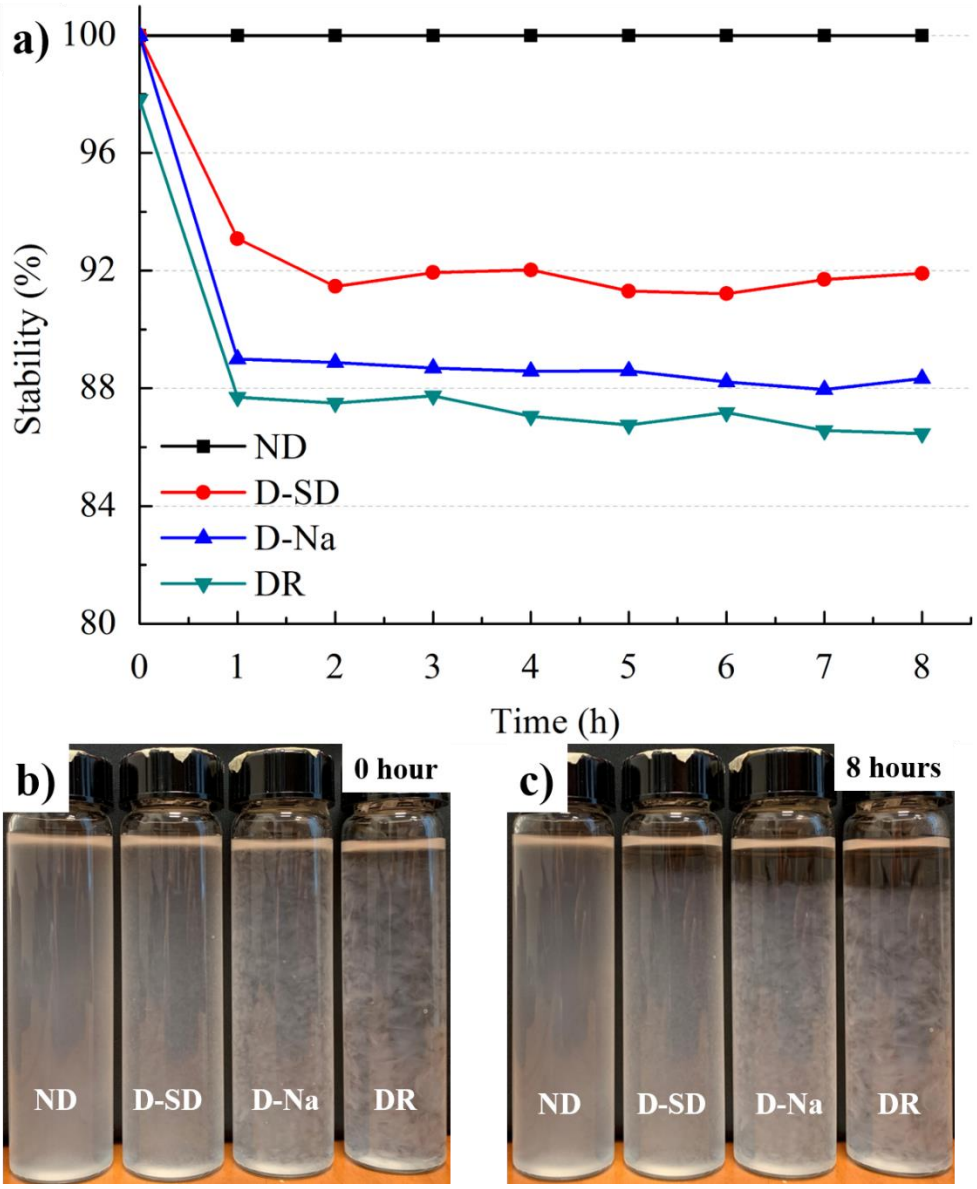


Figure 3: Stability in water for ND, D-SD, D-Na and DR (a); visual inspection and dispersion stability in 0 (b) and 8 (c) hours for all the four treatments.

All of the dried samples had shown sedimentation. All precipitation had occurred within the first hour for DR and D-Na and first 2 hours for D-SD. D-SD sample had kept its stability above 90%, being the most stable among the dried samples. No visible aggregate was present on D-SD, while D-Na sample had a final stability of approximately 88% but with visible clumps that were not dispersed during the process. DR was the least stable, with less than 87% of

stability with larger aggregates almost immediately precipitating (Figure 3). Due to the difficulty of measuring the meniscus of precipitated MFC, some oscillation was shown in D-SD sample. Nonetheless, it was worth noting that all dried samples had a high stability in water (>85% stability).

*3.3 Light microscopy*

After redispersing the freeze-dried samples, some persistent aggregation was present. In the case of the DR sample, mixing was not enough to separate the clumps which appeared as a woven-like structure of macrofibers through the light microscope (Figure 4).

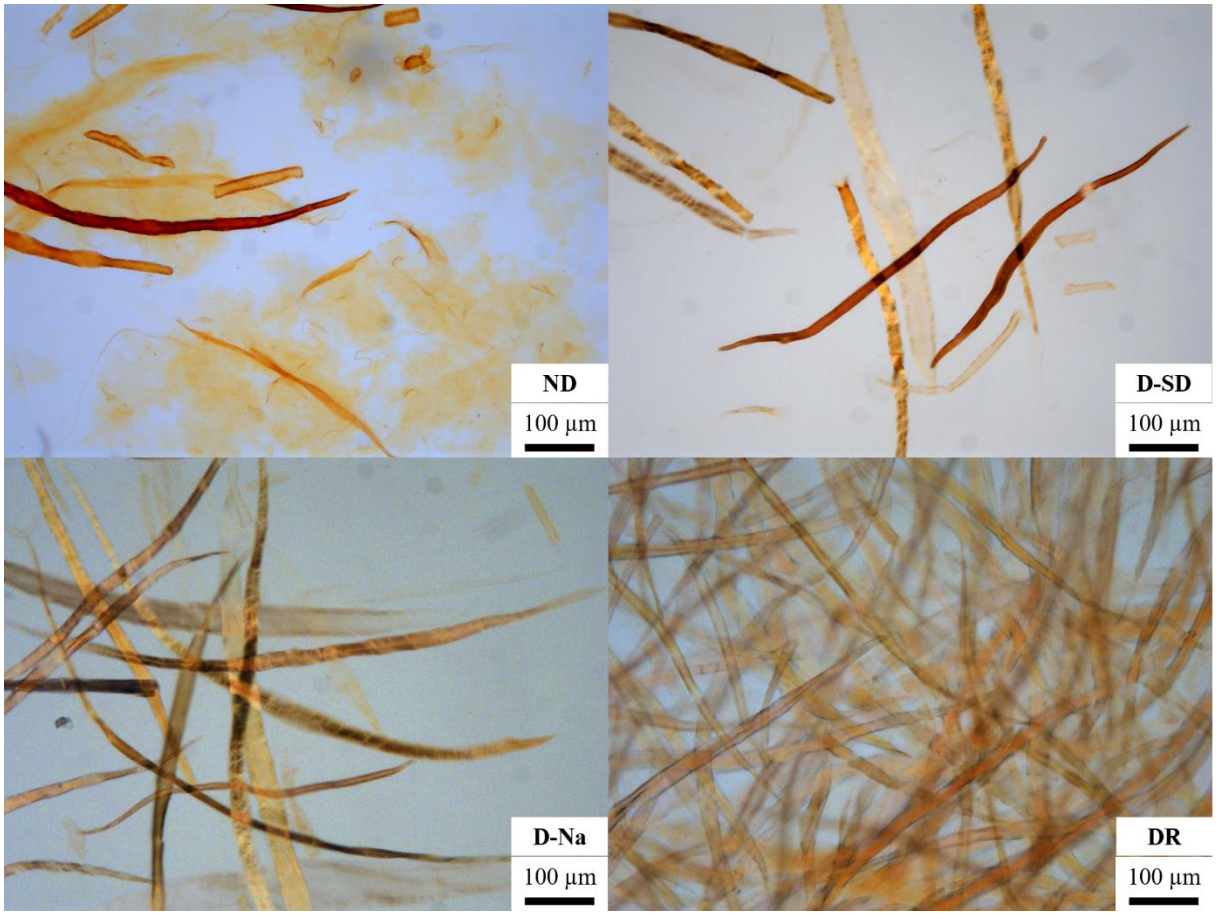


Figure 4: Light microscopy images of ND and freeze-dried samples D-SD, D-Na and DR, showing aggregation behavior.

The aggregates were visible macrofibers and linked together by concentrated MFC (Figure 3). D-Na and D-SD were easily dispersed, with fewer visible interlocked macrofibers. Because of this, the stability of the dispersion was higher when compared to DR. Not

surprisingly, ND did not present agglomeration caused by the drying process and showed the same macrofibers as the other treatments. This is a common occurrence on mechanically treat fibers (Tonoli et al., 2016; Guimarães Júnior et al., 2015; Tonoli et al., 2012).

*3.4 Scanning electron microscopy*

The morphology of freeze-dried samples is presented in Figure 5. In all of the individualized MFC or smaller bundles of fibrils, it was possible to notice twisting alongside the fiber. This chirality was caused by a variation on C6 carboxyl group in cellulose chains, which a change in proportion of trans-trans, trans-gauche and gauche-gauche conformations was responsible for realignment of the fibrils, as well as the effect of bound water and applied vacuum (Paajanen, Ceccherini, Maloney and Ketoja, 2019). Suspension concentration before drying seemed to be not necessary, because of the MFC-sheet formation (Han et al., 2013), especially for DR, that resembled oven dried MFC (Figure 5.a and b). However, D-Na and D-SD were able to hinder sheet formation, which was related to a was related to the inhibition of hydrogen bonding at the hydroxyl sites along the MFC chains, and D-SD still exhibited individualized MFC after lyophilization. With less contact in dry form, it was easier to disperse without aggregation. SDS micelles have the capability of bridging MFC, and in the present study, SDS (20 mM, 0.6wt%) was at a sufficiently low concentration not to destabilize MFC suspension (Quennouz et al., 2016) to cause charge screening, and unbalanced osmotic pressure, which would cause aggregation MFC (Xiang et al., 2019).

Images of D-SD samples revealed high porosity caused by ice-templating, which resulted in the MFC samples exhibiting a foam structure when freeze-dried (Antonini et al., 2019). The ice-templating mechanism occurred because of the growth of ice crystals in the dispersed water, during freezing (Medina et al., 2019; Antonini et al., 2019; Wang et al., 2019). This type of MFC foaming method creates voids inside the matrix providing great insulation properties (Wang et al., 2019). Here, SEM analysis corroborated with sedimentation analysis and light microscopy, proving that the addition of SDS was a more stable method to dry and redisperse MFC, compared to the addition of NaCl or no additives.

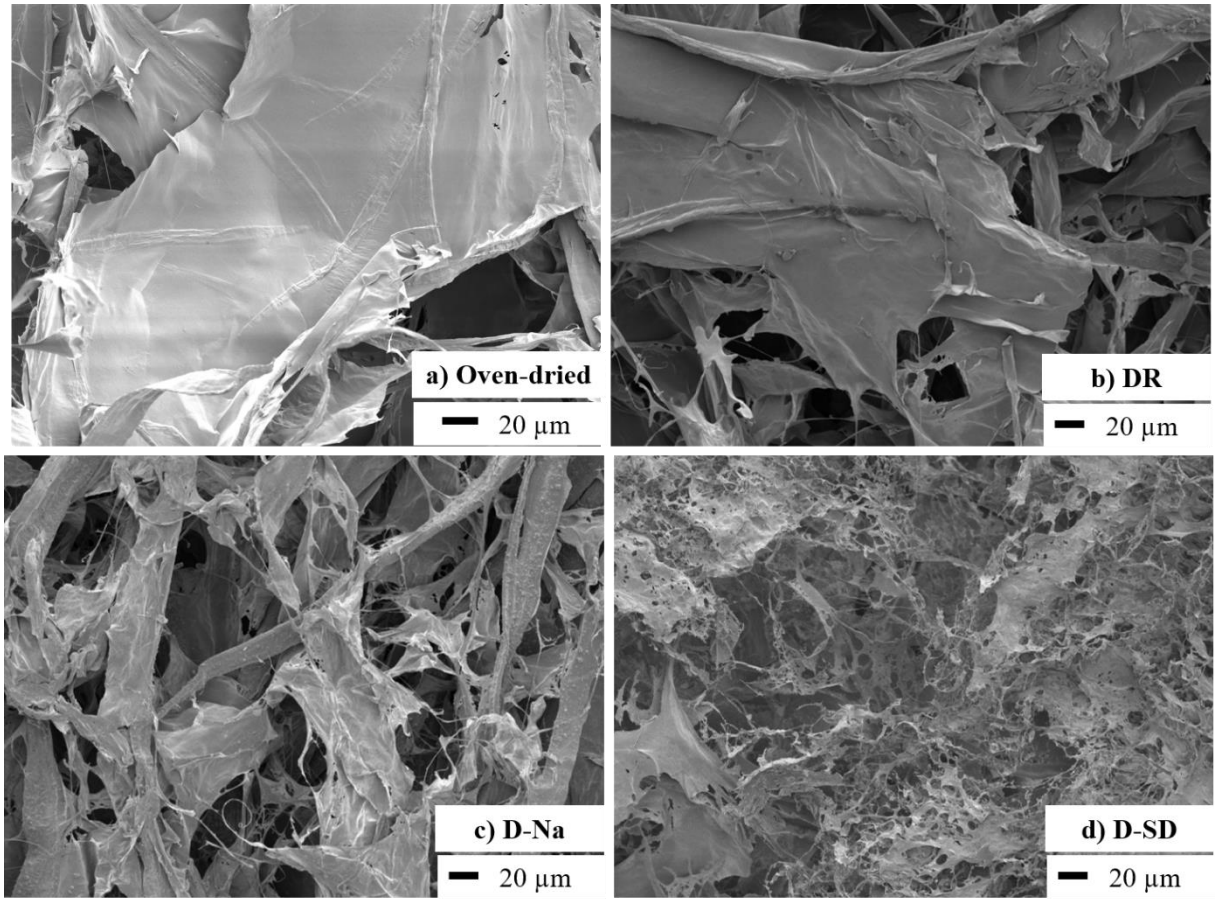


Figure 5: SEM images of samples surface morphology. a) Oven-dried MFC showing severe sheet-like structure during drying; and are freeze-dried samples with no additives (b), NaCl (c), and SDS (d).

*3.5 Particle size*

As discussed in previous sections, the difference in particle size of the redispersed samples was observed. The high capacity of MFC to interlock and form net-like structures, could enhance mechanical properties in the absence of aggregation (Butchosa and Zhou, 2014; Paakko et al., 2007). Figure 6 shows the particle size of the samples. When analyzing particles, light techniques project each measurement as an equivalent sphere, so it can be described with a single number (Rawle, 2003). In this method, the measurement is not from fiber diameter nor length, but the diameter of the assumed particle. In this case, the particle, when it reaches a significant size, is treated as an aggregate due to collapsing of multiples fibers and fragments into a bigger clump.

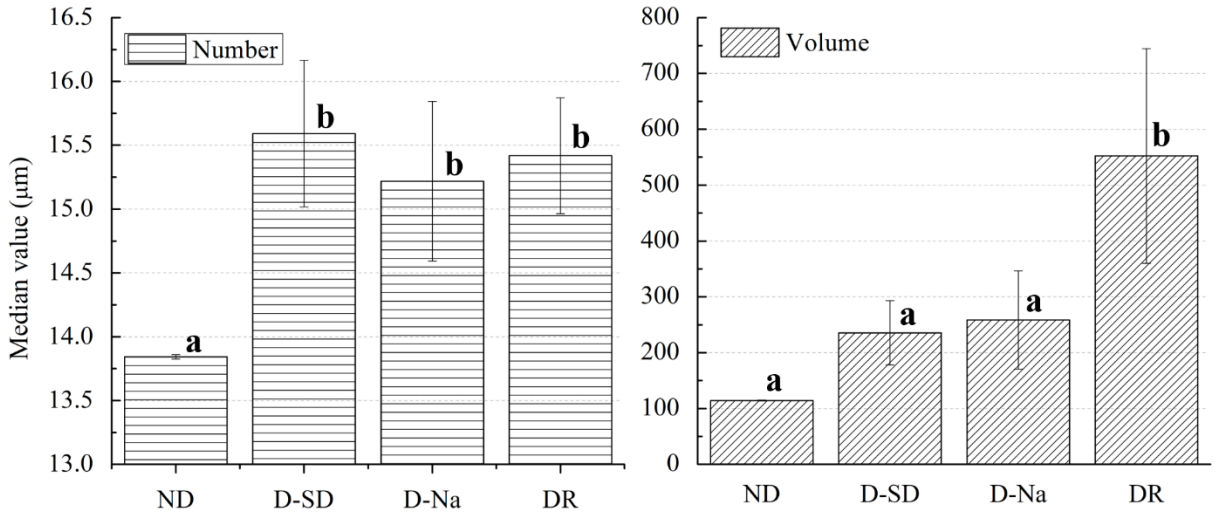


Figure 6: Average median size and standard deviation of MFC samples dispersed in water calculated by number and volume. Averages with the same letter, in the same graph, does not differ at 5% significance by Tukey test.

The samples D-SD and D-Na did not present any statistical difference from each another on both calculations. However, they both exhibited smaller particles compared to DR, based on volume measurements, and larger particles than ND, when calculated by number. The high value gap presented in DR is related to a vast size distribution, mainly from aggregates. Another mechanical treatment could possibly disperse DR better; however, further fibrillation could have happened (Benítez and Walther, 2017) and the present study aims to evaluate this easy and fast way to disperse MFC in all treatments. It is possible that another mechanical treatment could eliminate the aggregates (Benitez and Walther, 2017) and better disperse the DR sample. However, this present study was aimed at evaluating a more efficient method of dispersing MFC and the use of additives, and continued addition of mechanical treatments would fall beyond the scope of this work.

*3.6 Fourrier transformed infrared*

Fourrier transformed infrared (FTIR) spectroscopy was used to investigate chemical composition of the samples. As all treatments are made from the same material, the only changes would be expected was from unwashed additives. Since there was no chemical addition, and thus no difference between ND and DR, it was already expected that both spectra would be the same (Figure 7). All cellulose typical peaks were present. A broad band around 3300 $cm^{-1}$ was related to (-OH) stretching and intramolecular hydrogen bonding (Fauziyah,

Widiyastuti, Balgis and Setyawan, 2019), while 2891 $cm^{-1}$ (C-H) vibrations referred to methyl groups on cellulose chains. The range from 900 to 1150 $cm^{-1}$ was a region with characteristic (C-C) and (C-O) deformations inside the glycosidic ring (Luong et al., 2013). Due to TEMPO-mediated oxidation of the fibers, carboxyl groups were present at 1605 $cm^{-1}$ (Kassab et el., 2019), and was primarily a (C=O) vibration of sodium carboxylate (-COONa) MFC (Yang, Saito, Berglund and Isogai, 2015). The presence of NaCl is known to weaken cellulose intermolecular bonds (Missoum, Bras and Belgacem, 2012) or even influence on the tetrahedral formation of water molecules, distorting its shape (Seraji, Karimi, and Mahmoudi, 2017). Both situations' effect would be easily seen on 3300 $cm^{-1}$ FTIR broad halo. However, D-Na exhibited the same spectrum as ND and DR, indicating that the samples were thoroughly washed to remove any salt present.

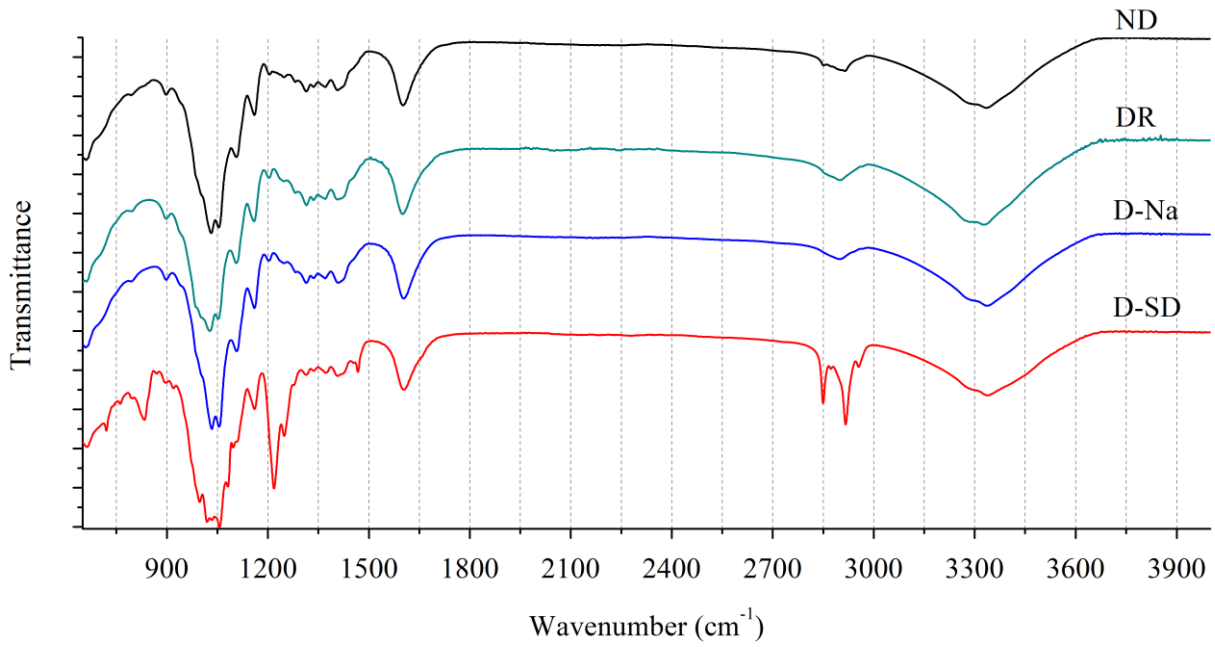


Figure 7: Typical FTIR spectra of ND, D-SD, D-Na and DR samples.

However, D-SD presented some changes, specially at two groups of wavelength: 1200-1250 $cm^{-1}$, which are responsible for $SO^{-2}$ asymmetric vibrations (Viana, Silva and Pimentel, 2012), and 2800-3000 $cm^{-1}$, which refer to the long alkyl chains of SDS (Suppiah, The, Husseinsyah and Rahman, 2019). Thus, sample rinsing was not as effective as expected for D-SD, leaving trace amounts of SDS on MFC.

*3.7 Mechanical properties*

Tensile strength and elongation are some reliable mechanical parameters used to investigate the presence of aggregates in the sample because the ability of forming a net-like structures are directly correlated to mechanical strength (Ioelovich, 2008). As expected, ND sample presented much higher elongation at break compared to DR samples (Figure 8 and Table 2). This happened because ND was never dried and, therefore, not submitted to any aggregation process during drying. With much less aggregates and more points of contact, the film was formed more evenly. Due to the presence of abundant points of contact between fibrils, when stress is applied, the drawing of the MFC permits the breakage of some hydrogen bonds that will allow sliding, without breaking, granting higher elongation at break (Butchosa and Zhou, 2014; Sehaqui et al. 2012).

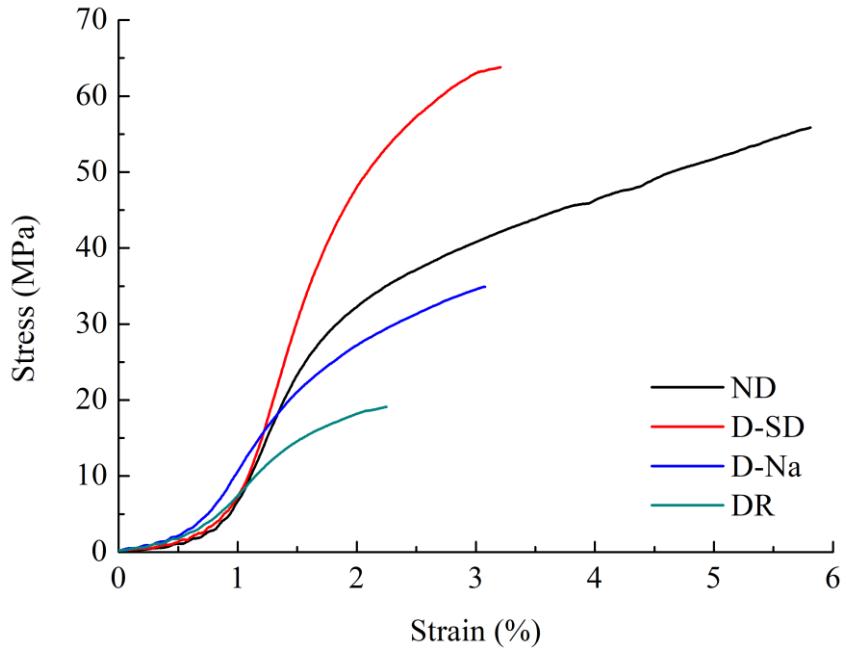


Figure 8: Typical stress-strain curves of ND, and D-SD, D-Na, and DR.

Table 2: Average and standard deviation of the mechanical properties of ND, D-SD, D-Na, and DR.

| Treatment | Young's modulus (GPa) | Elongation at break (%) | Maximum Stress (MPa) |
|---|---|---|---|
| ND | 5.0 ± 1.7 **b** | 7.6 ± 1.6 **a** | 54.0 ± 3.6 **a, b** |
| D-SD | 7.4 ± 2.7 **a** | 5.1 ± 1.4 **b** | 69.2 ± 22.6 **a** |
| D-Na | 4.3 ± 1.0 **b** | 4.1 ± 1.0 **b, c** | 36.6 ± 6.8 **b** |
| DR | 3.4 ± 0.6 **b** | 2.2 ± 0.5 **c** | 19.2 ± 2.9 **c** |

All means followed by the same letter does not differ at 5% significance.

On the other hand, tensile strength of D-SD was statistically higher than ND. This is because $Na^+$ ion from TEMPO-oxidation process can help bind the residual SDS onto the fibrils surface, creating a cross-linked network (Xiang et al., 2018) that increases tensile strength and Young's modulus. DR and D-Na exhibited loss in both elongation at break and tensile strength, indicating that the redispersion process did not result in maintaining the same properties for these two samples. This was probably due either to poor redispersion or irreversible aggregation, which could negatively impact mechanical strength. On the other hand, even though SDS caused MFC to become more brittle, its tensile strength was improved without significant loss in elongation. Again, this showed that using SDS in MFC dispersion before drying could not only produce easily-disperse stable samples, but also, enhance mechanical properties in the presence residual of SDS.

## 4 CONCLUSIONS

The effects of the use of additives during freeze-drying on the morphological, water stability, and mechanical behavior of MFC were investigated. Dried MFC was prepared via TEMPO-mediated oxidation of Eucalyptus fibers. The addition of NaCl aided to redisperse the MFC during the process, producing less aggregates compared to a dried control, and both did not suffer any chemical modification nor was any salt residue found after the process. Alternatively, using SDS not only promoted a well dispersed suspension, but also increased tensile strength and Young's modulus; however, it did exhibit some loss in elongation, which was caused by a residual presence of SDS in the matrix. The present study has presented an efficient method to produce MFC films using SDS as a hydrogen bonding inhibitor.

## ACKNOWLEDGMENTS

This study was financed in part by the Coordenação de Aperfeiçoamento de Pessoal de Nível Superior – Brasil (CAPES) – Finance Code 001.The authors also acknowledge the support of the Fundação de Amparo à Pesquisa do Estado de Minas Gerais – FAPEMIG, Conselho Nacional de Desenvolvimento Científico e Tecnológico – CNPq, and the Bioproducts Research Unit (BRU - ARS) at the United States Department of Agriculture (Albany - CA).

## REFERENCES

Antonini, C., et al. (2019). Ultra-Porous Nanocellulose Foams: A Facile and Scalable Fabrication Approach. *Nanomaterials, 9,* 1142.

Arantes, A. N. C., et al. (2019). Bio-based thin films of cellulose nanofibrils and magnetite for potential application in green electronics. *Carbohydrate Polymers, 207*, 100–107.

Ballesteros, J. E. M., Dos Santos, V., Mármol, G., Frías, M., & Fiorelli, J. (2017). Potential of the hornification treatment on eucalyptus and pine fibers for fiber-cement applications. *Cellulose, 24*, 2275-2286.

Benítez, A. J., & Walther, A. (2017). Cellulose nanofibril nanopapers and bioinspired nanocomposites: a review to understand the mechanical property space. *Journal of Materials Chemistry A, 5*, 16003-16024.

Claro, P. I. C., et al. (2018). Curaua and eucalyptus nanofibers films by continuous casting: Mechanical and thermal properties. *Carbohydrate Polymers, 181*, 1093–1101.

Cuissinat, C., Navard, P., & Heinze, T. (2008). Swelling and dissolution of cellulose. Part IV: Free floating cotton and wood fibres in ionic liquids. *Carbohydrate Polymers, 72*, 590-596.

Eyholzer, C., et al. (2010). Preparation and characterization of water-redispersible nanofibrillated cellulose in powder form. *Cellulose 17*, 19–30.

Fall, A. B., Lindström, S. B., Sundman, O., Ödberg, L., & Wågberg, L. (2011). Colloidal Stability of Aqueous Nanofibrillated Cellulose Dispersions. *Langmuir, 27*, 11332–11338.

Fauziyah, M., Widiyastuti, W., Balgis, R., & Setyawan, H. (2019). Production of cellulose aerogels from coir fibers via an alkali–urea method for sorption applications. *Cellulose, 26*, 9583 – 9598.

Fukuzumi, H., Tanaka, R., Saito, T., & Isogai, A. (2014). Dispersion stability and aggregation behavior of TEMPO-oxidized cellulose nanofibrils in water as a function of salt addition. *Cellulose, 21*, 1553–1559.

Gardner, D. J., Oporto, G. S., Mills, R., & Samir, M. A. S. A. (2008). Adhesion and surface issues in cellulose and nanocellulose. *Journal of Adhesion Science and Technology, 22*, 545–567.

Guimaraes Junior, M., Teixeira, F. G., & Tonoli, G. H. D. (2018). Effect of the nano-fibrillation of bamboo pulp on the thermal, structural, mechanical and physical properties of nanocomposites based on starch/poly (vinyl alcohol) blend. *Cellulose, 25,* 1823 – 1849.

Han, J., Zhou, C., Wu, Y., Liu, F., & Wu, Q. (2013). Self-assembling behavior of cellulose nanoparticles during freeze-drying: effect of suspension concentration, particle size, crystal structure, and surface charge. *Biomacromolecules*, *14*, 1529−1540.

Huan, S., et al. (2017). Formulation and Composition Effects in Phase Transitions of Emulsions Costabilized by Cellulose Nanofibrils and an Ionic Surfactant. *Biomacromolecules*, *18*, 4393−4404.

Ioelovich, M. (2008). Nanostructured cellulose: Review. *BioResources, 3*, 1403-1418.

Kassab, Z., et al. (2019). Production of cellulose nanofibrils from alfa fibers and its nanoreinforcement potential in polymer nanocomposites. *Cellulose, 26*, 9567 – 9581.

Liu, S., Yu, T., Wu, Y., Li, W., & Li, B. (2014). Evolution of cellulose into flexible conductive green electronics: a smart strategy to fabricate sustainable electrodes for supercapacitors. *RSC Advances, 4*, 34134–34143.

Lo, J., Yen, H., Tsai, C., Chen, B., & Hou, S. (2014). Interaction between Hydrophobically Modified 2-Hydroxyethyl Cellulose and Sodium Dodecyl Sulfate Studied by Viscometry and Two-Dimensional NOE NMR Spectroscopy. *The Journal of Physical Chemistry B, 118*, 6922−6930.

Luong, N. D., et al. (2013). Processable polyaniline suspensions through in situ polymerization onto nanocellulose. *European Polymer Journal, 49*, 335 – 344.

Medina, L., Carosio, F., & Berglund, L.A. (2019). Recyclable nanocomposite foams of Poly (vinyl alcohol), clay and cellulose nanofibrils – Mechanical properties and flame retardancy. *Composites Science and Technology, 182*, 107762.

Missoum, K., Bras, J., & Belgacem, M. N. (2012). Water redispersible dried nanofibrillated cellulose by adding sodium chloride. *Biomacromolecules, 13*, 4118−4125.

Osong, S. H., et al. (2016). Qualitative evaluation of microfibrillated cellulose using the crill method and some aspects of microscopy. *Cellulose, 23*, 3611–3624.

Paajanen, A., Ceccherini, S., Maloney, T., & Ketoja, J. A. (2019). Chirality and bound water in the hierarchical cellulose structure. *Cellulose, 26*, 5877–5892.

Pääkkö, M., et al. (2007). Enzymatic hydrolysis combined with mechanical shearing and high-pressure homogenization for nanoscale cellulose fibrils and strong gels. *Biomacromolecules, 8*, 1934-1941.

Patruyo, L. G., Müller, A. J., & Sáez, A. E. (2002). Shear and extensional rheology of solutions of modified hydroxyethyl celluloses and sodium dodecyl sulfate. *Polymer, 43*, 6481–6493.

Peng, Y., Gardner, D. J., & Han, Y. (2012). Drying cellulose nanofibrils: in search of a suitable method. *Cellulose, 19*, 91-102.

Phan-Xuan, T., et al. (2016). Aggregation behavior of aqueous cellulose nanocrystals: the effect of inorganic salts. *Cellulose, 23*, 3653–3663.

Quennouz, N., Hashmi, S. M., Choi, H. S., Kim, J. W., & Osuji, C. O. (2016). Rheology of cellulose nanofibrils in the presence of surfactants. *Soft Matter, 12*, 157 – 164.

Saito, T., & Isogai, A. (2004). TEMPO-Mediated Oxidation of Native Cellulose. The Effect of Oxidation Conditions on Chemical and Crystal Structures of the Water-Insoluble Fractions. *Biomacromolecules, 5*, 1983-1989.

Schindelin, J., et al. (2012). Fiji: an open-source platform for biological-image analysis. *Nature methods, 9*, 676-682.

Sehaqui, H., et al. (2012). Cellulose nanofiber orientation in nanopaper and nanocomposites by cold drawing. *ACS Applied Mater & Interfaces, 4*, 1043–1049.

Seraji, H. R., Karimi, M., & Mahmoudi, M. (2017). In situ monitoring the change of mechanical response induced by the diffusion of saline water in glassy cellulose acetate. *Desalination, 420*, 191-207.

Sim, G., Alam, M. N., Godbout, L., & Vem, T. (2014). Structure of swollen carboxylated cellulose fibers. *Cellulose, 21*, 4595 – 4606.

Suppiah, K., Teh, P. L., Husseinsyah, S., & Rahman, R. (2019). Properties and characterization of carboxymethyl cellulose/halloysite nanotube bio-nanocomposite films: Effect of sodium dodecyl sulfate. *Polymer Bulletin, 76*, 365–386.

TAPPI. (1994). Fines fraction of paper stock by wet screening (T 261 cm-94).

Tardy, B. L., et al. (2017). Nanocellulose–surfactant interactions. *Current Opinion in Colloid & Interface Science, 29*, 57–67.

Tonoli, G. H. D., et al. (2016). Properties of cellulose micro/nanofibers obtained from eucalyptus pulp fiber treated with anaerobic digestate and high shear mixing. *Cellulose, 23*, 1239–1256.

Wang, Q., et al. (2019). Processing nanocellulose to bulk materials: a review. *Cellulose, 26*, 7585–7617.

Xiang, X., et al. (2018). Foam processing of fibers as a sustainable alternative to wet-laying: fiber web properties and cause−effect relations. *ACS Sustainable Chemistry & Engineering, 6*, 14423−14431.

Xiang, W., et al. (2019). How Cellulose Nanofibrils Affect Bulk, Surface, and Foam Properties

of Anionic Surfactant Solutions. *Biomacromolecules, 20*, 4361 – 4369.

Yang, Q., Saito, T., Berglund, L. A., & Isogai, A. (2015). Cellulose nanofibrils improve the properties of all-cellulose composites by the nano-reinforcement mechanism and nanofibril-induced crystallization. *Nanoscale, 7*, 17957.

Zhang, X., et al. (2019). Redispersibility of cellulose nanoparticles modified by phenyltrimethoxysilane and its application in stabilizing Pickering emulsions. *Journal of Materials Science, 54*, 11713–11725.

Zimmermann, M. V. G., et al (2016). Drying techniques applied to cellulose nanofibers. *Journal of Reinforced Plastics and Composites, 35*, 682–697.

## PART IV – FINAL CONSIDERATIONS

This manuscript has achieved the conclusion of two distinct studies involving MFC redispersion and its consequent changes. The first one evaluated the structural and morphological changes of MFC promoted by drying/redispersion cycles at different temperatures. The results have shown that both number of cycles and temperatures changes the aggregation behavior of the samples. The aggregation process happened more harshly with higher temperatures (75 and 100°C) and most cycles (C5), while room temperature once-dried samples (C1 - 20°C) remained similar to never-dried MFC (MFC-Control), both in morphology and structure.

On the second study, the effects of the use of additives during freeze-drying on the morphological, water stability, and mechanical behavior of MFC were investigated. The addition of NaCl and SDS had helped produced more easily dispersible samples, being SDS the best additive. SDS presented the same characteristics as the never-dried MFC (ND), but a trace amount of the additive left in the sample had increased considerably mechanical properties, which made this, the best method.

In both studies, redispersion process were evaluated and the results indicate that the best way of drying MFC without losing its properties is to use less cycles, lower temperature or use SDS as an additive.